

The geology of Gona, Afar, Ethiopia

Jay Quade

Department of Geosciences, University of Arizona, Tucson, Arizona 85721, USA

Naomi E. Levin

Department of Geology and Geophysics, University of Utah, Salt Lake City, Utah 84112, USA

Scott W. Simpson

Department of Anatomy, Case Western Reserve University School of Medicine & Laboratory of Physical Anthropology, Cleveland Museum of Natural History, Cleveland, Ohio 44106, USA

Robert Butler

Department of Physics, University of Portland, Portland, Oregon 97203-5798, USA

William C. McIntosh

New Mexico Bureau of Geology and Mineral Resources, New Mexico Institute of Mining and Technology, Socorro, New Mexico 87801, USA

Sileshi Semaw

CRAFT Stone Age Institute, Indiana University, 1392 West Dittmore Road, Gosport, Indiana 47433-9531, USA

Lynnette Kleinsasser

Department of Geosciences, University of Arizona, Tucson, Arizona 85721, USA

Guillaume Dupont-Nivet

Department of Earth Sciences, Utrecht University, Budapestaan 17, 3584 CD Utrecht, The Netherlands

Paul Renne

Berkeley Geochronology Center, 2455 Ridge Road, Berkeley, California 94709, USA

Nelia Dunbar

Department of Earth and Environmental Science, New Mexico Institute of Mining and Technology, Socorro, New Mexico 87801, USA

ABSTRACT

Deposits in the Gona Paleanthropological Research Project (GPRP) area in east-central Ethiopia span most of the last ~6.4 m.y. and are among the longest and most complete paleoenvironmental and human fossil archives in East Africa. The $^{40}\text{Ar}/^{39}\text{Ar}$ and paleomagnetic dates and tephrostratigraphic correlations establish the time spans for the four formations present at Gona: the Adu-Asa (>6.4–5.2 Ma), Sagantole (>4.6–3.9 Ma), Hadar (3.8–2.9 Ma), and Busidima Formations (2.7 to <0.16 Ma). The volcano-sedimentary succession at Gona displays many classic tectono-sedimentary features of an evolving rift basin. The mixed volcanic and fluviolacustrine Adu-Asa Formation is the earliest expression of rifting at Gona, probably deposited in a small half-graben. The Sagantole and Hadar Formations were deposited in a much

larger half-graben bounded to the E-NE by an as-yet-unidentified normal fault. The Sagantole and Hadar Formations are both fluvial and lacustrine, reflecting periodic shallow impoundment of a low-gradient paleo-Awash River, perhaps by an accommodation zone north of the Ledi-Geraru project area.

Starting at 2.9–2.7 Ma, the character of sedimentation changed dramatically throughout the Awash Valley as bed load coarsened and the meandering paleo-Awash River cyclically cut and filled. Unlike the Hadar Formation, the Busidima Formation thickens westward, suggesting deposition in a half-graben of the opposite polarity compared to Sagantole/Hadar time. Sedimentation rates decreased 5-fold, from 0.25 mm/yr in the Hadar Formation to 0.05 mm/yr in the Busidima Formation, perhaps in response to slowing extension rates and/or opening of the half-graben north of Gona.

Keywords: Gona, Ethiopian Rift, tephrostratigraphy, Busidima, Sagantole, Adu-Asa.

REGIONAL SETTING AND SCOPE OF STUDY

The Gona Paleoanthropological Research Project (GPRP) area lies at 11°N on the western flank of the southern Afar Rift, transitional between the Ethiopian Rift to the south and the rest of the Afar Rift to the north. East-west rifting between the Nubian and Somali plates flanking the rift commenced ca. 18 Ma and propagated northward into the southern Afar by ca. 11 Ma (WoldeGabriel et al., 1990). The Awash Valley today follows the Awash half-graben (see Fig. 7 of Wynn et al. [this volume] for a valleywide cross section), which is the most recent (younger than 2.9 Ma) structural expression of rifting in the Gona Paleoanthropological Research Project. The As Duma fault is the most significant structural feature of the project area, marking the western edge of the Awash half-graben. The As Duma fault divides the western half of Gona, underlain by the Adu-Asa and Sagantole Formations, from the younger Hadar and Busidima Formations, which occur largely east of the fault (Fig. 1). Even though faulting and minor volcanism remain active at Gona and surrounding project areas, the area of maximum extension and volcanism associated with the rift currently lies ~100 km to the east, along the Wonji fault belt (Bilham et al., 1999; Chernet et al., 1998).

The Gona Paleoanthropological Research Project encompasses ~130 km² of deeply dissected badlands produced by deep incision by the Awash River and its tributaries (Fig. 1). The Awash River, which marks the southeastern boundary of the project area, originates to the south in the Ethiopian highlands and follows the rift north past the study area before turning east and terminating in Lake Abhe in the Goba'ad graben. The Hadar Formation (3.8–2.9 Ma), exposed in the Hadar project area north of Gona, first attracted paleoanthropologists in the 1970s, when it yielded a rich array of fossils (e.g., Gentry, 1981; Johanson et al., 1982), including well-known examples of *Australopithecus afarensis* and *Homo* sp. (Johanson and Taieb, 1976; Kimbel et al., 1994). Research spanning several decades has established the main outlines of the geology of the Hadar Formation (Taieb et al., 1976; Aronson and Taieb, 1981; Tiercelin, 1986; Aronson et al., 1977; Walter and Aronson, 1982, 1993; Walter, 1994; Campisano and Feibel, this volume, Chapters 6 and 8).

Fossil-rich deposits both younger and older than the Hadar Formation (3.8–2.9 Ma) are much less studied but well represented at Gona and are the main focus of this paper. These include the Adu-Asa Formation (>6.4–5.2 Ma), the Sagantole Formation (>4.6–3.9 Ma), and the newly designated Busidima Formation (2.7 to <0.16 Ma) (Quade et al., 2004) (Fig. 2). The stratigraphy and geochronology of the Adu-Asa Formation are the topics presented by Kleinsasser et al. (2008) in this volume, whereas, in this paper, we touch only upon the sedimentology and regional structural context of the Adu-Asa Formation. The Sagantole Formation lies stratigraphically above the Adu-Asa Formation and has been largely unstudied until now, despite its rich fossil record including *Ardipithecus ramidus*. The Sagantole Formation is extensively faulted, and thus only small areas around the richest fossil sites have been documented in detail and are presented here. Finally, the Busidima Formation rests unconformably upon the Hadar Formation. In a previous paper (Quade et al., 2004), we presented the results of our study of the age, stratigraphy, and sedimentology of this newly designated formation. In this paper, we update those results and present new chronologic evidence from the tephtras and paleomagnetic zones in all the formations. We also report on newly explored areas in the upper half of the Busidima Formation, an area rich in archaeology and hominid remains. We end the paper by placing the geologic history of Gona into the larger tectono-stratigraphic context of the Ethiopian Rift, and by merging carbon isotopic evidence from paleosols (Quade et al., 2004; Levin et al., 2004) and fossil teeth (Levin et al., this volume) with sedimentologic evidence to reconstruct the paleoenvironments of hominids through time at Gona.

METHODS

Tephra Analysis

Tephtras were first treated with 2 M HCl to remove any carbonate, briefly rinsed in 2% HF, washed in distilled water, and sieved. In most cases, the 60–120 μm size fraction was used for electron microprobe analyses. All analyses were made on a CAMECA SX50 electron microprobe with a wavelength-

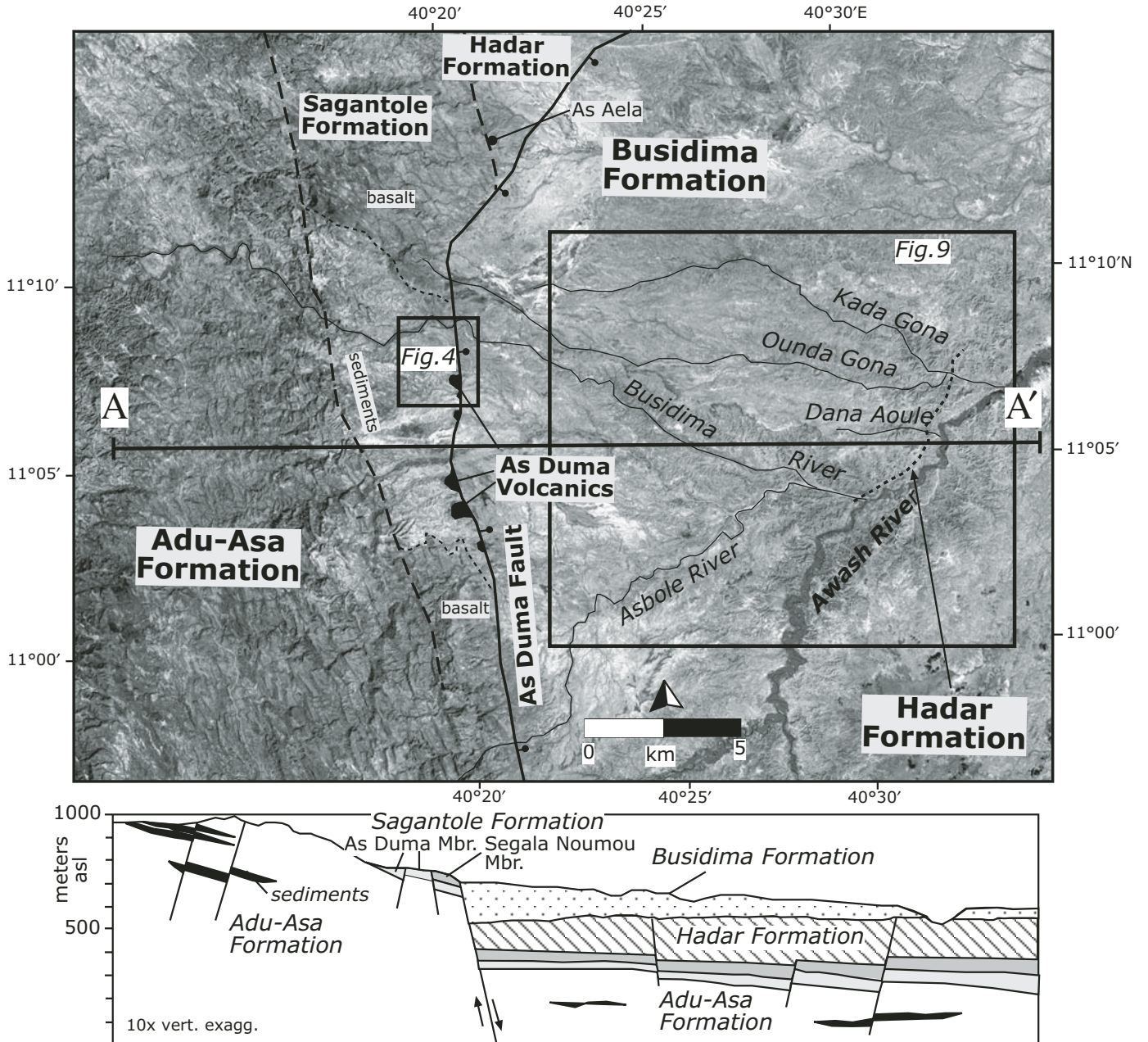


Figure 1. Regional view of the geology of Gona, with geologic cross section below. The contact between the Busidima and Hadar Formations (coarse dotted line) is only shown for the Gona project area. Areas of the Sagantole Formation dominated by basalt and sediments are separated by fine dotted lines. All formations beneath the Busidima Formation (the Hadar [see Wynn et al., this volume], and especially the Sagantole and Adu-Asa) are probably normally faulted and tilted east of the As Duma fault, but these faults cannot be located on this cross section with certainty.

dispersive spectrometry system at the University of Arizona, Department of Planetary Sciences Lunar and Planetary Laboratory. Calibrations were performed daily using simple silicate minerals and synthetic oxides.

Sodium and potassium volatilization during electron microprobe analyses of glass is widely recognized and depends on the intensity, diameter, and duration of the incident electron beam (Nielsen and Sigurdsson, 1981; Hunt and Hill,

1993). Initially, all elements were run at 15 KeV, 20 nanoamps, and 2 μm beam diameter. To minimize volatilization in later sample runs, we changed analytical conditions for alkalis to 8 nanoamps and a beam diameter of 10 μm . All results with analytical totals less than 90% were excluded. Normalization of oxide composition to 100% is undesirable, as it may mask poor analyses, resulting in an increased chance of false correlation of tephras (Hunt and Hill, 1993).

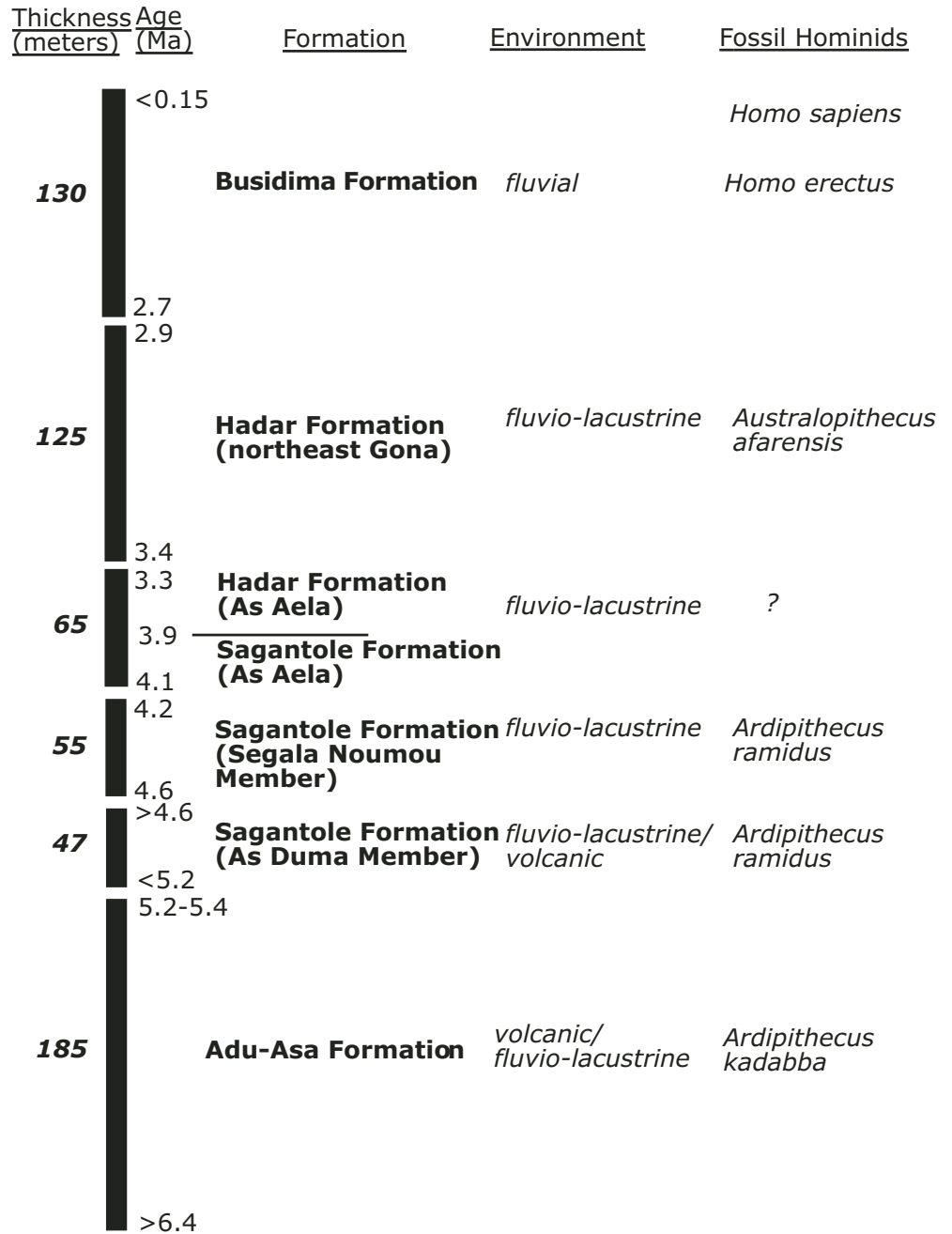


Figure 2. Estimated ages, thicknesses, and depositional environments of major formations at Gona, along with fossil hominids represented at Gona and other north Awash project areas.

Paleomagnetic Dating

Claystone and siltstone layers were sampled for paleomagnetic analyses. Three to five oriented samples were collected from each sedimentary horizon. Over 70 sites were collected and analyzed (Table DR1¹) from the Sagantole Formation, and from the Busidima Formation along the Dana Aoule and Busidima

drainages. Most samples were cored in situ with a modified hole saw driven by a portable electric drill. Orientation of core samples was done using standard methods (Butler, 1992). Samples from sedimentary layers too fragile for coring were collected as oriented blocks that were later trimmed into core-shaped samples using a hand rasp. All samples were stored, measured, and thermally demagnetized in a magnetically shielded room with average field intensity <200 nanotesla (nT). Natural remanent magnetization (NRM) was measured using a three-axis cryogenic magnetometer (2G Model 755R). Typical NRM intensities ranged from 10⁻¹ to 10⁻² A/m. After

¹GSA Data Repository item 2008216, stratigraphic sections and dating results, is available at www.geosociety.org/pubs/ft2008.htm, or on request from editing@geosociety.org, Documents Secretary, GSA, P.O. Box 9140, Boulder, CO 80301-9140, USA.

initial NRM measurements, samples were subjected to progressive thermal demagnetization at 12–15 temperatures up to 580 °C, where most samples retained <5% of initial NRM. Typical thermal demagnetization behaviors are illustrated in Figure DR10 (see footnote 1). Dominant unblocking temperatures distributed below 580 °C suggest that the NRM is carried by detrital magnetite and that the primary NRM is a depositional remanent magnetism.

Principal component analysis of NRM remaining at four to eight successive temperature steps between 400 °C and 580 °C was used to determine the characteristic remanent magnetization (ChRM) (Kirschvink, 1980). Samples yielding maximum angular deviation (MAD) >15° were rejected from further analysis. Site-mean ChRM directions were determined using methods of Fisher (1953) and examined using the test for randomness of Watson (1956). Sites with three or more samples yielding ChRM directions that were nonrandom at the 5% significance level were designated class A sites. Sites with two or more samples with more dispersed ChRM directions but unambiguous polarity were designated class B sites. Sites yielding only one sample ChRM direction or two samples with highly dispersed directions of ChRM were rejected from further analysis. Class A and B sites are listed in Table DR1 (see footnote 1) and were used to construct the magnetic polarity columns.

⁴⁰Ar/³⁹Ar Dating

Single plagioclase crystals separated from GONASH-14, -16, -21, -39, -41, -51, and -52 (Table 1) were dated by ⁴⁰Ar/³⁹Ar using the methods and facilities at the Berkeley Geochronology Center (California, USA) described by Renne et al. (1998). The rest of the samples listed in Table 1 were analyzed at New Mexico Geochronology Research Laboratory (Socorro, New Mexico, USA) following procedures described in McIntosh and Chamberlin (1994). Reported ages are based on 28.02 Ma for the Fish Canyon sanidine standard (Renne et al., 1998), which yields ages ~0.7% older than the calibration employed by WoldeGabriel et al. (1994) and Renne et al. (1999), and errors are reported at the 2σ level. Full presentation and discussion of Ar/Ar data are given in Table DR2 and Figure DR11 (see footnote 1). In all, 16 new dates can be added to the 11 previously published dates from the Sagantole, Hadar, and Busidima Formations at Gona (Table 1). Kleinsasser et al. (this volume) describe the geochronology of the Adu-Asa Formation.

GEOLOGIC HISTORY

Adu-Asa Formation

The oldest hominid-bearing unit at Gona is the Adu-Asa Formation (Fig. 1). It is at least 185 m thick and spans the time period between >6.4 and 5.2 Ma (Kleinsasser et al., this volume). The Adu-Asa Formation is dominated by ridge-forming basalts that form uplands on the western side of the study area, inter-

bedded with variably thick packages of sediments. This distinctive formation can be readily traced southward out of Gona, into the Middle Awash project area, where the Adu-Asa Formation was first studied (Kalb et al., 1982).

Sediments dominate the middle portion of the Adu-Asa Formation and are separated into an upper and lower sequence by a distinctive 5-m-thick porphyritic basalt flow (Kleinsasser et al., this volume, their Fig. 12). The lower sequence consists of ~90 m of pale-green to gray-brown laminated (Fl) to massive (Fm) clay and mudstone, interbedded with trough cross-bedded litharenite (St) and minor conglomerate (mostly Gm) (Fig. 3A) (notation modified from Miall, 1978). Fish fossils, plant fragments, and altered pumice are present in some laminated clays. White to yellow chert, 30 to 50 cm thick, is locally present in the claystone. Gray (unaltered) to white and yellow (altered) tephra are common; some, such as the Sifi and Kobo'o tephra, serve as key stratigraphic marker beds (Kleinsasser et al., this volume). Some whitish layers rich in fish fossils appear to be altered diatomite. The conglomerates consist entirely of volcanic clasts, with roughly equal proportions of basaltic and felsic volcanics. We interpret this lower sedimentary sequence to be lacustrine (fish fossil-rich laminated siltstone, chert) below the level of the Sifi tephra and fluvial (conglomerates, trough cross-bedded sandstone, and tan siltstone) above it.

The upper sedimentary sequence is ~65 m thick, and it consists of massive pale-brown siltstone (Fm) interbedded with volcanoclastic sandstone and numerous basalt flows. Tephra are common—among them, a sequence of pumiceous, obsidian-rich tephra known as the Belewa tephra, and the Ogoti ash-flow complex near the top of the formation. The upper sedimentary sequence seems to be entirely fluvial, with no evidence of the lacustrine conditions seen in the lower sedimentary sequence.

Basalt in the Adu-Asa Formation occurs mostly as flows with minor basaltic air-fall tephra. Typical flow morphologies include vesicular chill bases and tops, and pahoehoe textures on the paleosurface. Flows vary in thickness from 1 to 10 m. In the basalt-dominated upper portion of the Adu-Asa Formation, stacked flows are visible, often divided by 0.5–2-m-thick bright red silty layers, which we interpret as intraflow paleosols (Fig. 3B). Kleinsasser et al. (this volume) have also identified one silicic eruptive center, called the Ogoti volcanic complex, near the top of the section.

The Adu-Asa Formation is rich in mammalian fossils, including the remains of *Ardipithecus kadabba* (Simpson et al., 2007). The fossiliferous horizons occur in three stratigraphic levels: the lowest (ABD-1, -2; HMD-1) in lacustrine sediments below the level of the Sifi and the Bodele (6.48 ± 0.22 Ma) tephra. Another group is found (BDL-1, -2, HMD-2) in fluvial sandstone and possible conglomerate ~10–15 m above the Bodele tephra, and a third group (ESC-1, -2, -3, -8, -9) is slightly higher in the section at or just below the Kobo'o tephra level (5.45 ± 0.07 Ma) in both fluvial sandstone and laminated siltstone (Table 2) (Kleinsasser et al., this volume).

TABLE 1. $^{40}\text{Ar}/^{39}\text{Ar}$ DATES FROM GONA

Sample	L#	Irrad	Min	Plateau (step-heat) or mean (SCLF) age*		Isochron age		MSWD	n	MSWD	$^{40}\text{Ar}/^{39}\text{Ar}$ (Ma, $\pm 2\sigma$)	Age (Ma, $\pm 2\sigma$)	Age (Ma, $\pm 2\sigma$)	Comments
				n	% ^{39}Ar	MSWD	Age (Ma, $\pm 2\sigma$)							
Sagantole Fm.														
GONNL 3	55438-01	NM-186J	Plagioclase	6	66.8	5.6	5.14 \pm 0.27	6	6.8	297.8 \pm 12.5	5.11 \pm 0.34			Hada Tuff, As Duma Mbr.
GONASH-51 [#]	31200		Plagioclase	23	NA	NA	4.56 \pm 0.23	NA	NA	NA	NA	NA	NA	Tuff, middle Segala Nourmou Mbr.
GONASH-52 [#]	31202		Plagioclase	16	NA	NA	4.60 \pm 0.46	NA	NA	NA	NA	NA	NA	Tuff, middle Segala Nourmou Mbr.
GON05 275	55977-01	NM-192H	Plagioclase	7	89.5	3.9	4.63 \pm 0.18	7	4.1	300.1 \pm 11.1	4.42 \pm 0.33			Hada Tuff, As Duma Mbr.
WMASH 15	56273-01	NM-196J	Plagioclase	5	66.0	3.4	4.66 \pm 0.11	5	1.9	258.0 \pm 32.2	4.91 \pm 0.22			Purple tuff locality, Segala Nourmou Mbr.
WMASH-25 [#]	56251-01	NM-196F	Plagioclase	9	92.6	1.0	4.47 \pm 0.04	9	1.0	294.1 \pm 3.5	4.48 \pm 0.05			Purple tuff locality, Segala Nourmou Mbr.
WMASH-27 [#]	52560-01	NM-141	Groundmass	7	90.6	1.5	4.17 \pm 0.21	9	3.3	297.7 \pm 1.6	4.05 \pm 0.17			Basaltic dike cutting flow below GWM-5
WMASH 43	52558-01	NA	Groundmass	7	86.6	3.4	4.06 \pm 0.39	7	7.5	298.0 \pm 3.0	4.00 \pm 0.30			Basaltic dike cutting flow below GWM-5
WMASH 47**	56252-01	NM-196G	Plagioclase	11	99.9	1.3	4.23 \pm 0.05	11	1.5	295.0 \pm 4.3	4.23 \pm 0.06			Tuff, top of Segala Nourmou Mbr.
WMASH 48	56253-01	NM-196G	Groundmass	0	0.0	0.0	0.00 \pm 0.00	8	20.1	300.0 \pm 11.4	1.77 \pm 1.28			Basalt flow, As Duma Mbr.
WMASH 49	57138-01	NM-208D	Groundmass	6	80.8	1.4	3.58 \pm 0.31	6	1.7	297.0 \pm 5.7	3.44 \pm 0.61			Basaltic dike cutting flow below GWM-5
WMASH 50	56255-01	NM-196G	Groundmass	8	93.2	0.9	4.17 \pm 0.12	8	1.3	297.8 \pm 6.5	4.13 \pm 0.17			Basaltic dike cutting flow below GWM-5
WMASH 55	56254-01	NM-196G	Groundmass	7	93.9	2.5	4.29 \pm 0.26	7	2.6	292.9 \pm 5.5	4.43 \pm 0.38			Basaltic dike cutting flow below GWM-5
WMASH 59	57140-02	NM-208D	Groundmass	8	99.7	2.4	3.97 \pm 0.33	8	2.8	296.6 \pm 6.8	3.88 \pm 0.64			Basalt flow capping the Sagantole Fm.
WMASH 62**	57135-01	NM-208C	Groundmass	9	100.0	1.4	4.42 \pm 0.22	9	1.6	296.8 \pm 4.7	4.23 \pm 0.73			Corestone, Barsuli Hill
WMASH 70	56256-01	NM-196G	Groundmass	6	54.9	1.4	4.42 \pm 0.27	6	0.6	301.4 \pm 5.2	3.45 \pm 0.87			Corestone, Baruli Hill
WMASH 65	57175	NM-2085	Sanidine	8	89.7	1.8	4.35 \pm 0.07	8	1.9	293.8 \pm 4.3	4.37 \pm 0.09			Yellow tuff at GWM-31
Hadar Fm.				12	NA	2.3	4.10 \pm 0.07	12	2.3	500.0 \pm 500.0	4.07 \pm 0.12			Tuff, base of As Aela
GONNL 68	55992	NM-192K	Sanidine	9	NA	0.6	3.27 \pm 0.10	9	0.8	296.0 \pm 3.0	3.26 \pm 0.20			Tuff, top of As Aela
BKT-2L [†]	7201		Anorthoclase	21	NA	NA	2.94 \pm 0.01	NA	NA	NA	NA	NA	NA	Tuff, Kada Gona
Busidima Fm.														
GONASH-79	56259	NM-196H	Sanidine	7	NA	1.4	1.90 \pm 0.10	7	1.4	320.0 \pm 50.0	1.83 \pm 0.18			Tuff, Ounda Gona south
GONASH-14 [§]	NA		Sanidine	25	NA	NA	2.53 \pm 0.31	NA	NA	NA	NA	NA	NA	Tuff, Fialu
GONASH-16 [§]	NA		Plagioclase	14	NA	NA	1.64 \pm 0.03	NA	NA	NA	NA	NA	NA	Tuff, Fialu
GONASH-21 [§]	NA		Sanidine	26	NA	NA	2.17 \pm 0.18	NA	NA	NA	NA	NA	NA	Tuff, Ounda Gona north
GONASH-39 [§]	NA		Sanidine	17	NA	NA	2.69 \pm 0.06	NA	NA	NA	NA	NA	NA	Tuff, Dana Aoule
GONASH-41 [§]	NA		Plagioclase	22	NA	NA	2.27 \pm 0.28	NA	NA	NA	NA	NA	NA	Tuff, Dana Aoule
AST-2.75 [†]	8302		Plagioclase	23	NA	NA	2.52 \pm 0.15	NA	NA	NA	NA	NA	NA	Tuff, Kada Gona

Notes: Ages were calculated relative to FC-2 Fish Canyon Tuff sandine interlaboratory standard (28.02 Ma; Renne et al., 1998). Analyses were performed at New Mexico Geochronology Research Laboratory using an MAP 215-50 mass spectrometer on line with automated all-metal extraction system. All errors are reported at $\pm 2\sigma$, unless otherwise noted. Details of irradiation, analytical procedures, calculation methods, and analytical data are in Table DR2 and Figure DR11 (see text footnote 1).

*Single-crystal laser fusion (SCLF) dates are in italics.

[†]Published in Semaw et al. (1997).

[§]Published in Quade et al. (2004).

[#]Published in Semaw et al. (2005).

**Shaded text denotes unreliable dates.

Sagantole Formation

The Sagantole Formation crops out continuously in the western half of the Gona Paleoanthropological Research Project area, resting conformably(?) on the Adu-Asa Formation to the west, and bounded to the east by the As Duma fault (Fig. 1). The type area for the Sagantole Formation is the central complex of the Middle Awash Project area (see volume introduction), where deposits of overlapping age and similar lithology are present (Kalb et al., 1982; Renne et al., 1999). In all, the Sagantole Formation at Gona covers an area of ~3 km × 30 km. Reconnaissance of this large area reveals that sediments make up >70% of the Sagantole Formation, interbedded with the remnants of cinder cones such as those at Umele Delti and around fossil site GWM-5 (Fig. 4). To the north and south of Gona, sediments of the Sagantole Formation grade laterally into stacked basalt flows (Fig. 1).

Sedimentary strata in the Sagantole Formation are all deformed and tilted gently to the E/NE at ~5°–10°. The entire area is cut by normal faults with offsets varying from less than a meter to tens of meters. The faults are oriented mostly NW-SE, sub-parallel to the As Duma fault (Fig. 4), but dip either east or west. The numerous faults made mapping and correlation of strata between fault blocks very difficult. Moreover, Quaternary-age gravels eroded in part from the prominent basalt ridges of the Adu-Asa Formation to the east have covered large tracts of the Sagantole Formation, preventing tracing of outcrops between areas.

At least one major interformational normal fault, the Segala Noumou fault, cuts through the Sagantole Formation from NW to SE (Fig. 4). The fault juxtaposes largely pale-colored fluvio-lacustrine sediments, which we newly designate the Segala Noumou Member of the Sagantole Formation (Fig. 4, Tl and Tu), to the east against much redder lacustrine, volcanoclastic and locally fanglomeratic sediments of the As Duma Member to the west (Fig. 4, Tr). Previously, in Semaw et al. (2005), we referred to the As Duma Member as the “WM-5 block,” and the Segala Noumou Member as the “WM-3 block.” The sediments of the As Duma Member appear to be older than those in the Segala Noumou Member to the east, based on their redder color, greater induration, and abundance of interlayered volcanic rocks. However, as we discuss later, geochronologic evidence points to both younger and older ages for the As Duma Member. Resolution of this apparent contradiction is important, as the Sagantole Formation on both sides of the Segala Noumou fault contains abundant remains of *Ardipithecus ramidus*, but only those to the east of the fault (Segala Noumou Member) can be firmly dated. In this paper, we concentrate on fossil-bearing sediments of both the Segala Noumou and As Duma Members bounded by the Busidima River on the north and the Sifi River on the south. Outside this area, the Sagantole Formation remains largely unstudied geologically at Gona.

Segala Noumou Member

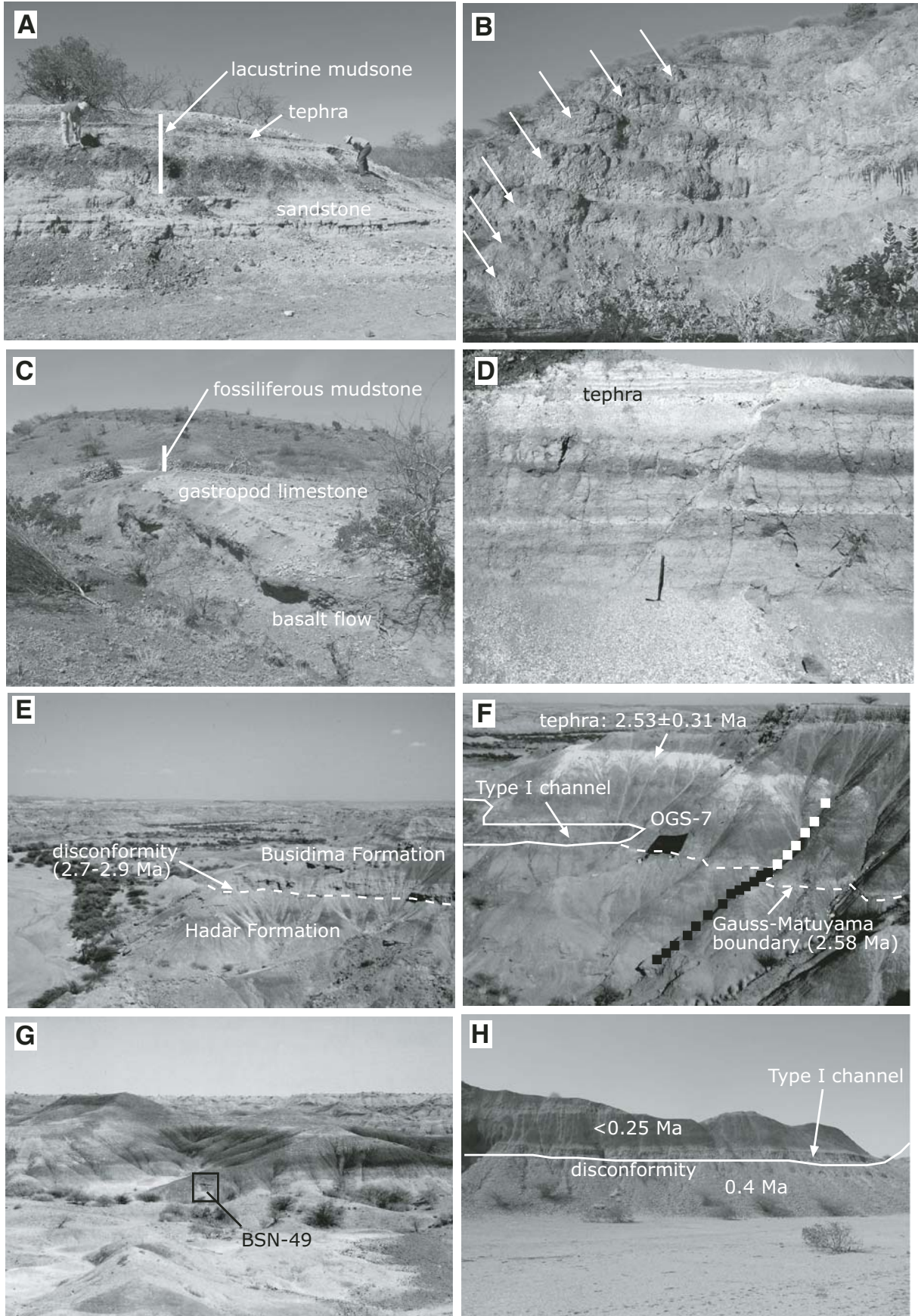
Sediments of the Segala Noumou Member are bounded by the Segala Noumou fault to the west and the As Duma fault to the east (Fig. 4). The section is a minimum of 40 m thick,

to which we can add at least another 15–20 m of unmeasured section near the As Duma fault. The Segala Noumou Member consists of pale-brown to green laminated (Fl) to massive (Fp) siltstone and cross-bedded sandstone (St or Sr) interbedded with minor conglomerates (Gm), altered tephra, and densely cemented carbonate tufas (Fig. 5; see Miall [1978] for notation). Table 3 summarizes the features of these deposits and their environmental interpretation. In general, the laminated, fish fossil-rich siltstones can be viewed as lacustrine, the massive calcareous siltstones as paleosols, the sandstones as fluvial and possibly deltaic (containing aquatic mollusks *Bellamya* sp., *Cleopatra* sp., *Biomphalaria* sp., *Melanoides tuberculata*, and Unionids), and the conglomerate as fluvial. Three lacustrine intervals appear to be represented in the Segala Noumou Member, two lower intervals dominated by fissile shale and an upper one represented by gastropod-rich (*Cleopatra* sp.) tufas, which can be traced across the middle of the member, suggesting shallow lake or paludal conditions (Fig. 5). Mammalian fossils are common in these tufas (Fig. 5, GWM-3, -3sw) or occur in bedded siltstone (Fh) possibly representing overbank deposits (Fig. 5, GWM-67). The conglomerates and sandstones are generally less than a few meters thick, and the bed forms are small, implying small-scale rivers and creeks. The conglomerates contain a mix of volcanic clasts cemented by sparry calcite.

Ash-fall tephra within the Segala Noumou Member are yellow to white in the field and vary in thickness from a few centimeters to over a meter. All show complete alteration of glass, and some show alteration of plagioclase phenocrysts, when present. Unlike the As Duma Member, the sediments of the Segala Noumou Member are not volcanoclastic, except at the base, and are not interbedded with flows or coarse cinder.

Geochronologic evidence from the Segala Noumou Member suggests that it ranges in age from 4.6 to 4.2 Ma. Dates on plagioclase from four air-fall tephra in the lower lacustrine interval range from 4.47 ± 0.04 Ma to 4.66 ± 0.11 Ma (Table 1, WMASH-15, -16, GONASH-51, -52). A fifth tephra (Table 1, WMASH-70) near fossil site GWM-31 (Fig. 4) in fluvial sediments, perhaps in the upper part of the Segala Noumou Member, produced an age of 4.35 ± 0.07 Ma. A final date from a tephra in the stratigraphically highest position in the Segala Noumou Member next to the As Duma fault is 4.23 ± 0.05 Ma (Table 1, WMASH-43; Fig. 4). The exact stratigraphic thickness dividing this sample from dated intervals lower in the member (shown in Fig. 5) is not known but is probably on the order of 15–20 m. A basalt flow (Table 1, WMASH-55), found resting on sediments of the Segala Noumou Member and possibly a part of the As Duma volcanics (Fig. 4), produced an age of 3.97 ± 0.33 Ma.

We sampled for magnetostratigraphy from 14 overlapping sites covering ~20 m of sedimentary thickness (Fig. 5). Paleomagnetic polarity directions from all samples are reversed, consistent with $^{40}\text{Ar}/^{39}\text{Ar}$ dates, which span 4.66 ± 0.11 – 4.23 ± 0.05 Ma. This range falls largely within magnetozones C3n.1r, a period of reversed magnetic polarity spanning 4.51–4.32 Ma (Lourens et al., 2004). Since we did not



sample paleomagnetically at the very base or top of the Segala Noumou Member, our interpretation is that this member spans 4.6–4.2 Ma. The key fossil-bearing localities in the Segala Noumou Member all cluster in the lower two-thirds of the sequence. GWM-67 is the lowest site stratigraphically (Fig. 5; column WM06-14) and dates to ca. 4.5 Ma. GWM-3, -3w (Fig. 5; column WM99-1; see also Semaw et al., 2005), and perhaps GWM-31 are slightly younger at 4.3–4.4 Ma.

As Duma Member

Sedimentary and volcanic rocks in the As Duma Member of the Sagantole Formation crop out west of the Segala Noumou fault. Lithologically, this member is extremely varied, from thick sequences of reddish fanglomerates and interbedded sandstone in some areas, to mud-dominated reddish siltstone elsewhere. We only measured sections immediately west of the Segala Noumou fault where thicknesses exceed 40 m (Fig. 6). Deposits in this area are sedimentologically very similar to those of the Segala Noumou Member, except for the presence of a basaltic cone and associated flows and dikes at the base of the measured section (Fig. 3C) and abundant volcanoclastic debris laterally (Fig. 3D). The debris consists of fine cinder, agglutinated spatter, accretionary lapilli, and volcanic bombs in laminated siltstone. A

gastropod-rich limestone dominated by the aquatic snail *Melanoides tuberculata* lies directly on the basalt (Fig. 3C), overlain by reddish-purple silt and claystone full of fine cinder (Fig. 3D). The clay and siltstone are bioturbated at the base and laminated higher in the section. Fish fossils and tiny gastropods similar to *Gyraulus* sp. are common. We interpret this sequence to represent onlapping and deepening of a paleolake onto the flanks of a small, active cinder cone. Above 22 m (Fig. 6), the remainder of the section is dominated by fluvial conglomerates, sandstone, bedded overbank siltstone, and reddish paleosols.

Fossil mammalian remains, including those of *Ardipithecus ramidus*, are abundant in the cindery siltstone immediately above the gastropod-rich limestone (Figs. 7A and 7B; Semaw et al., 2005). We interpret this fossil-bearing horizon to represent a very shallow-water lacustrine setting on the flanks of an active basaltic cinder cone. Fossil sites GWM-1, -2, -5 series, and -9 all occur in this context (Fig. 7; Table 2).

For dating, we focused our efforts in the As Duma Member on the basaltic cinder cone and plagioclase from two tephra in the lacustrine sediments burying the cone. The cone consists of basaltic pyroclastic debris cut by dikes and surrounded by multilobe flows. Much of the basalt is palagonitized, making dating very difficult. The dikes and middle portion of the flows presented the densest, least altered, and least vitreous samples for dating, from which seven $^{40}\text{Ar}/^{39}\text{Ar}$ dates were obtained. Three (Table 1; WMASH-26, -47, -48) showed disturbed spectra and were dropped from further consideration. The four remaining dates (Table 1; WMASH-25, -27, -49, -50) yielded reasonably coherent plateau ages between 4.06 ± 0.39 Ma and 4.29 ± 0.26 Ma. Tephra sample by WMASH-28 contained too few radiogenic plagioclase phenocrysts for a meaningful date. The Hada tephra, although from lacustrine sediments stratigraphically above the basalt and the fossil sites, contained plagioclase that yielded ages of 5.14 ± 0.27 Ma (Table 1, GONNL-3) at one location and 4.53 ± 0.18 Ma (GON05-275) at another. We obtained magnetic polarity orientations from 10 sites taken from the basal basalt flow and from the overlying volcanoclastic siltstone. All of the polarity orientations are reversed (Fig. 6).

Taken together, the evidence places the As Duma Member below the Segala Noumou Member (older than 4.6 Ma) and above the Adu-Asa Formation (younger than 5.2 Ma). The geologic evidence shows that the As Duma and Segala Noumou Members do not overlap stratigraphically. Moreover, the As Duma fault appears to dip eastward, placing the As Duma Member in the footwall and making it older. We view the dates (5.14–4.53 Ma) from the Hada tephra as the most reliable indication of the age of the upper As Duma Member. All the basalts showed some degree of alteration, even the dike corestones that seemed to yield reliable ages. We originally (Semaw et al., 2005) assigned the As Duma Member to C3n.1r (4.50–4.30 Ma), the same period of reversed magnetic polarity spanning the Segala Noumou Member. However, the results from the Hada tephra point to an age older than 4.6 Ma, and therefore correlation would be with reversed polarity intervals

←

Figure 3. (A) Fluviolacustrine sediments at Hamadi Das (see Fig. 12 of Kleinsasser et al., this volume) from the lower half of the Adu-Asa Formation at the level of the Sifi tephra. Mammalian remains from this interval include *Ardipithecus kadabba*. (B) Layered basalt flows from the upper Adu-Asa Formation near the Belewa tephra (see Fig. 2 of Kleinsasser et al., this volume). At least seven distinct flows (arrows) are visible, separated by reddish (due partly to baking) paleosol; outcrop is ~25 m high. (C) Gastropod-rich limestone (white) resting on a basalt flow (~2.5 m thick in this photograph) in the As Duma Member of the Sagantole Formation. See Figure 6 for section description near this location. The dark-colored mudstones immediately above the limestone are rich in mammalian fossils, including multiple remains (GWM-5, 5s, 5SW) of *Ardipithecus ramidus* discussed in Semaw et al. (2005). (D) Laminated lacustrine claystone from the As Duma Member of the Sagantole Formation. These deposits grade laterally into the basalt flow shown in C. Note normal fault. The deposits are highly tuffaceous, including the white bed at the top of the photo; hammer is 1.2 m long. (E) Contact as exposed at Ounda Gona (Fig. 1) between the underlying Hadar Formation and overlying Busidima Formation. The contact is defined by the first appearance of type I channel gravels (shown) deposited by the coarse meandering ancestral Awash River. (F) Exposure along the Fialu (Fig. 9) of the OGS-7 archaeological site (under canvas, along with date on tephra [white layer]) and magnetic polarity directions (black square—normal; white square—reversed) of sediment. The site rests on a sand bank lateral to a major type I gravel of paleo-Awash River. Outcrop is ~35 m high. (G) Location (in box) of hominid site BSN-49 (see Fig. 9 for location) on top of Type II channel gravels in floodplain siltstone typical of the Busidima Formation at Gona between ca. 1.3 and 0.5 Ma; dark layer is a histic (organic-rich) zone within a paleosol near the top of the fining-upward sequence. (H) Return of type I gravels (the paleo-Awash River) near the top of the Busidima Formation along the Asbole River (Fig. 1). This channel system contains abundant Late (?) Stone Age artifacts and cuts over 35 m down into older sediments containing Acheulian artifacts. Outcrop height is ~8 m.

TABLE 2. AGES AND CONTEXTS OF MAJOR FOSSIL AND ARCHAEOLOGICAL LOCALITIES AT GONA

Site name	Site type (tool-making tradition)	Age (Ma)	Context
<u>Adu-Asa Formation</u>			
ESC-1	Fossil	5.5–6.0	Fluviolacustrine
ESC-2	Fossil	5.5–6.0	Fluviolacustrine
ESC-3	Fossil	5.5–6.0	Fluviolacustrine
ESC-8	Fossil	5.5–6.0	Fluviolacustrine
ESC-9	Fossil	5.5–6.0	Fluviolacustrine
BDL1	Fossil	6.2–6.4	Fluvial
BDL2	Fossil	6.2–6.4	Fluvial
ABD1	Fossil	6.2–6.4	Lacustrine
ABD2	Fossil	6.2–6.4	Lacustrine
HMD-1	Fossil	6.2–6.4	Lacustrine
HMD-2	Fossil	6.2–6.4	Fluvial
<u>Sagantole Formation</u>			
<u>Segala Noumou Member</u>			
GWM-3, -3w	Fossil	4.3–4.4	Paludal
GWM-67	Fossil	4.5	Fluvial
GWM-31	Fossil	4.3–4.4	Fluvial
<u>As Duma Member</u>			
GWM-1	Fossil	>4.6	Marginal lacustrine
GWM-2	Fossil	>4.6	Marginal lacustrine
GWM-5 series	Fossil	>4.6	Marginal lacustrine
GWM-9n	Fossil	>4.6	Marginal lacustrine
GWM-16	Fossil	>4.6	Marginal lacustrine
<u>Member uncertain</u>			
GWM-10	Fossil	As Duma Mbr.?	Marginal lacustrine
GWM-11	Fossil	As Duma Mbr.?	Marginal lacustrine/fluvial
GWM-45	Fossil	Segala Noumou Mbr. ?	Fluvial
GWMS-6	Fossil	Segala Noumou Mbr. ?	Paludal
GWMS-7	Fossil	Segala Noumou Mbr. ?	Paludal
GWMS-11	Fossil	Segala Noumou Mbr. ?	Paludal
<u>Busidima Formation</u>			
OGS 6/7	Archaeological (Oldowan)	2.5–2.6	Type I (Awash mainstem)
DAN 1,3	Archaeological (Oldowan)	2.5–2.6	Type I (Awash mainstem)
BSN-6	Archaeological (Oldowan)	2.5–2.6	Type I (Awash mainstem)
EG-10, -12, -13, -24	Archaeological (Oldowan)	2.5–2.6	Type I (Awash mainstem)
WG-5	Archaeological (Oldowan)	2.2	Type I (Awash mainstem)
OGN-3	Archaeological (Oldowan)	2.1	Type I (Awash mainstem)
OGS-3	Archaeological (Oldowan)	2	Type I (Awash mainstem)
BSN-12	Fossil and archaeological (Acheulian)	1.5–1.7	Type I–II
BSN-40	Fossil	1.5–1.7	Type I (Awash mainstem)
BSN-49	Fossil	0.9–1.4	Type II (Awash tributary)
BSN-65	Fossil	1.2–1.3	Type II (Awash tributary)
BSN-17	Archaeological (Acheulian)	1.5–1.7	Type I–II
OGS-12	Archaeological (Acheulian)	1.5–1.6	Type II (Awash tributary)
OGS-5	Archaeological (Acheulian)	1.4–1.5	Type II (Awash tributary)
DAN-5	Fossil and archaeological (Acheulian)	1.5–1.7	Type I (Awash mainstem)
DAN-16	Archaeological (Acheulian)	1.0–1.1	Type I (Awash mainstem)
ABE-1	Archaeological (Acheulian)	0.6	Type I (Awash mainstem)
GAN-10	Archaeological (Acheulian)	0.25	Type II (Awash tributary)
YAN-1	Fossil and archaeological (Acheulian?)	0.4	Type II (Awash tributary)
GWS-2	Archaeological (Acheulian?)	0.4	Type II (Awash tributary)
YAS-1	Archaeological (Late Stone age?)	<0.05?	Type I (Awash mainstem)

C3n.2r (4.80–4.63 Ma) or C3n.3r (4.90–5.00). The geologic, radiometric, and paleontologic evidence (Semaw et al., 1997) certainly precludes the As Duma Member from being younger (i.e., younger than 4.2 Ma) than the Segala Noumou Member. Nevertheless, we regard dating of the As Duma Member as work in progress. The key to resolving this question will be dating of more felsic tephras from the As Duma Member, and magnetostratigraphic sampling of longer sections.

As Duma Volcanics

The As Duma volcanics consist of a series of dikes, flows, and cinder cones that are aligned along the As Duma fault (Fig. 1). Virtually all of the volcanics are basaltic in composition. Palagonitic alteration of the basalt is very common, suggesting extensive interaction with surface water and groundwater during and after emplacement.

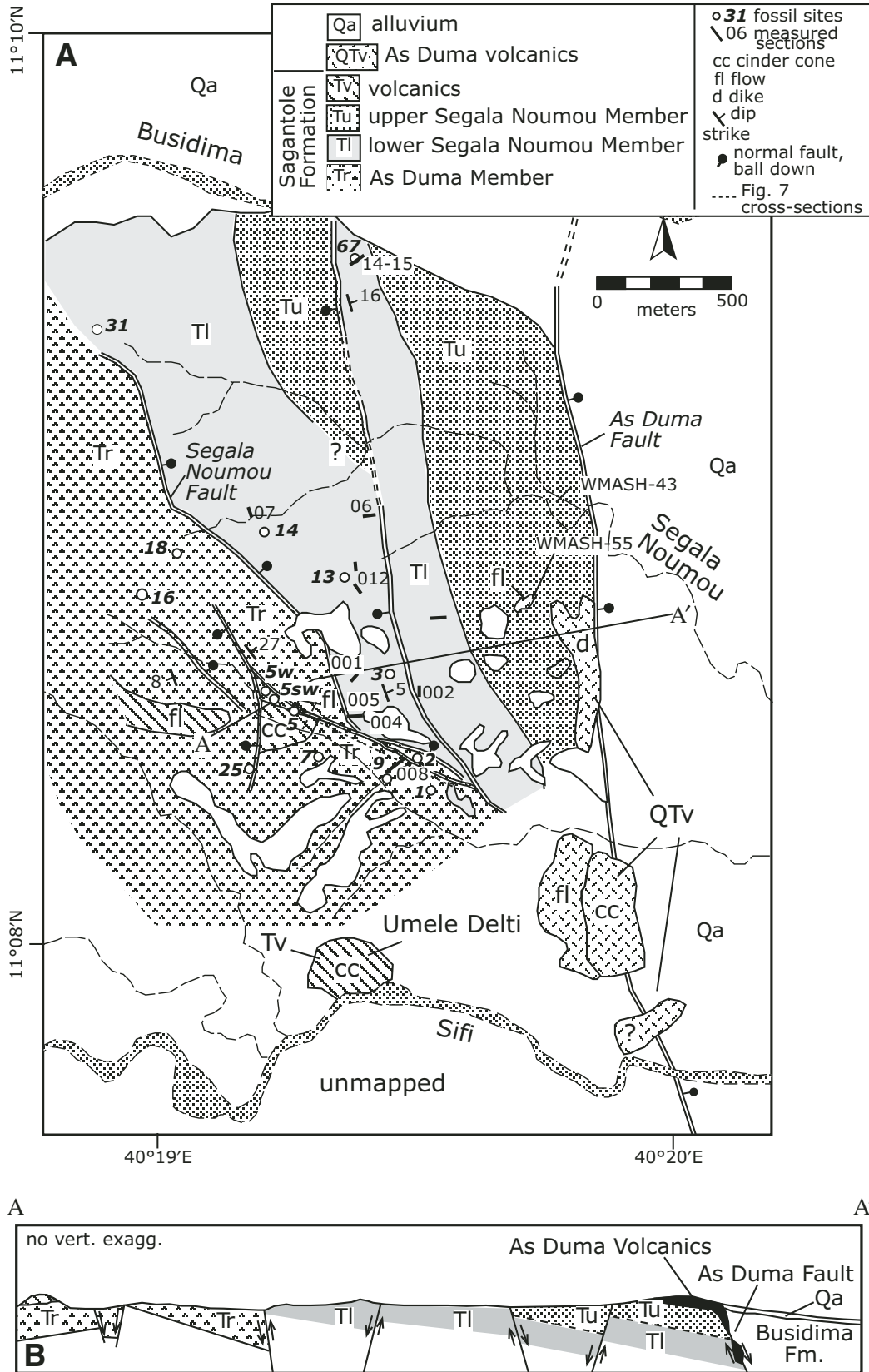


Figure 4. (A) Map and (B) cross section of the Sagantole Formation between the Busidima and Sifi. See Figure 1 for location of map area.

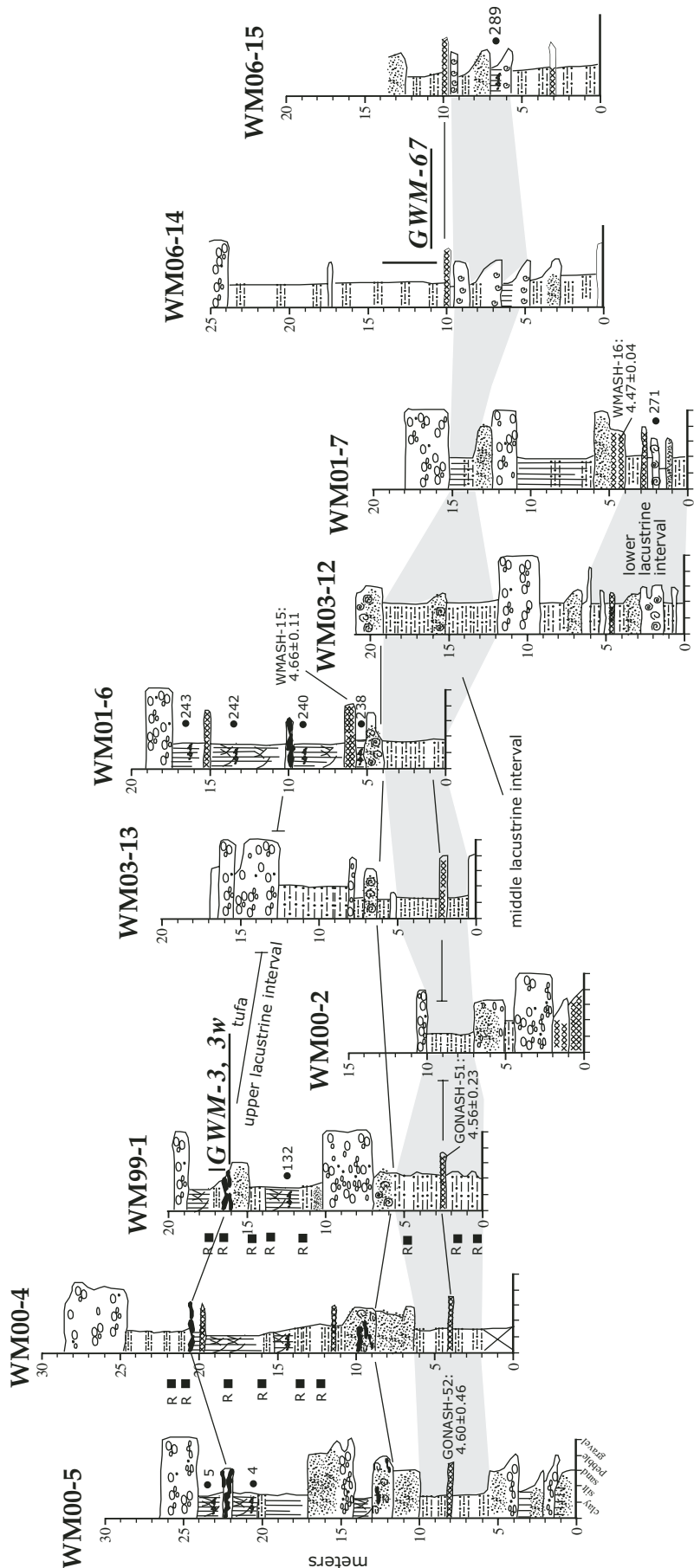


Figure 5. Measured stratigraphic sections within the Segala Noumou Member of the Sagantole Formation between the Busidima and Sifi. See Figure 4A for section locations and Figure 6 for legend.

TABLE 3. DEPOSITIONAL FEATURES OF THE SAGANTOLE FORMATION

Lithology	Symbol	Sedimentary features	Color	Fossils	Paleoenvironment
Silt or mudstone	F1	Laminated, fissile	Pale green	Fish, plants, crocodiles, mollusks	Lacustrine
Silt or mudstone	Fh	Laminated to bedded, stained with hydrojarosite	Pale brown	Mammalian fossils	Floodplain overbank
Silt or mudstone	Fm	Slickensides, subhorizontal cracks, carbonate nodules and rhizoliths	Brownish red	Absent	Vertic paleosol
Sandstone	Sr or St	Ripple (Sr) or trough (St) cross-bedded	Light gray	Mollusks (<i>Bellamyia</i> sp., <i>Biomphalaria</i> sp., <i>Melanooides tuberculata</i> , Unionids), reworked fossils	Fluvial or fluviodeltaic
Conglomerate	Gm	Massive	Dark gray	Absent	Fluvial
Tufa	Cm	Massive	Tan	Mollusks, mammalian fossils	Shallow lacustrine or paludal

Geologic relationships suggest that the As Duma volcanics all postdate 2.9 Ma, the age of the top of the Hadar Formation, but are not actively forming today. The main evidence for this is the alignment of the As Duma volcanics along the As Duma fault, which itself cuts the Sagantole Formation and Hadar Formations. The antiquity of the As Duma volcanics is supported by field evidence that suggests to us that volcanic activity has ceased or slowed along this reach of the As Duma fault. The cinder cones are deeply eroded and do not retain their original form. Dikes are cut by the As Duma fault, as apparent from their exposure only in the footwall of the fault. The presence of two (Table 4; samples BUSTASH-9/17 [BBT tephra] and ASASH-13) basaltic tephtras in the younger Busidima Formation (2.7 to <0.15 Ma) hints at continued basaltic volcanic activity at some location in or close to the Gona Paleoanthropological Research Project area, perhaps from along the As Duma fault.

Hadar Formation

The Hadar Formation crops out in two areas of the Gona Paleoanthropological Research Project: One is along the Awash River in the easternmost portion of the project area, where the Awash River has cut down through the overlying Busidima Formation, exposing up to 125 m of the formation (Fig. 1). The other area of exposure is west of the As Duma fault in the As Aela area (Fig. 1), where the Hadar Formation rests directly on the Sagantole Formation.

The Hadar Formation has undergone extensive study over the past 30 yr (e.g., Aronson et al., 1977; Tiercelin, 1986; Walter, 1994; Yemane, 1997; Campisano et al., this volume, Chapter 8; Wynn et al., this volume), and the portions exposed along the lower Kada Gona have already been discussed in Quade et al. (2004). We present the full stratigraphic logs for that study in Figure DR2 (see footnote 1). In brief, the Hadar Formation at Gona and in the neighboring Hadar and Dikika areas consists of four members, in ascending order: the Basal, Sidi Hakoma, Denen Dora, and Kada Hadar Members. At Gona, deposition spans ca. 3.8–2.9 Ma, and the lower boundary exposed at As Aela is conformable with the Sagantole Formation, whereas the upper contact with the overlying Busidima Formation is marked by an angular unconformity.

Like the Sagantole Formation, the Hadar Formation along the Awash River is characterized by several laminated shale intervals rich in fossil mollusks and fish, representing at least three lacustrine transgressions into the Gona area between ca. 3.5 and 2.9 Ma. The lacustrine intervals are interbedded with fluvial-deltaic sands, overbank siltstones, and vertic paleosols (Quade et al., 2004).

At least 65 m of newly identified strata straddling the Sagantole-Hadar Formation contact are reported here for the first time. The As Duma fault turns to the northeast near the northern boundary of the project area, cutting upsection through the entire Sagantole Formation and exposing the lower and Hadar Formation (Fig. 1). Beds dip at ~7°–10° to the east.

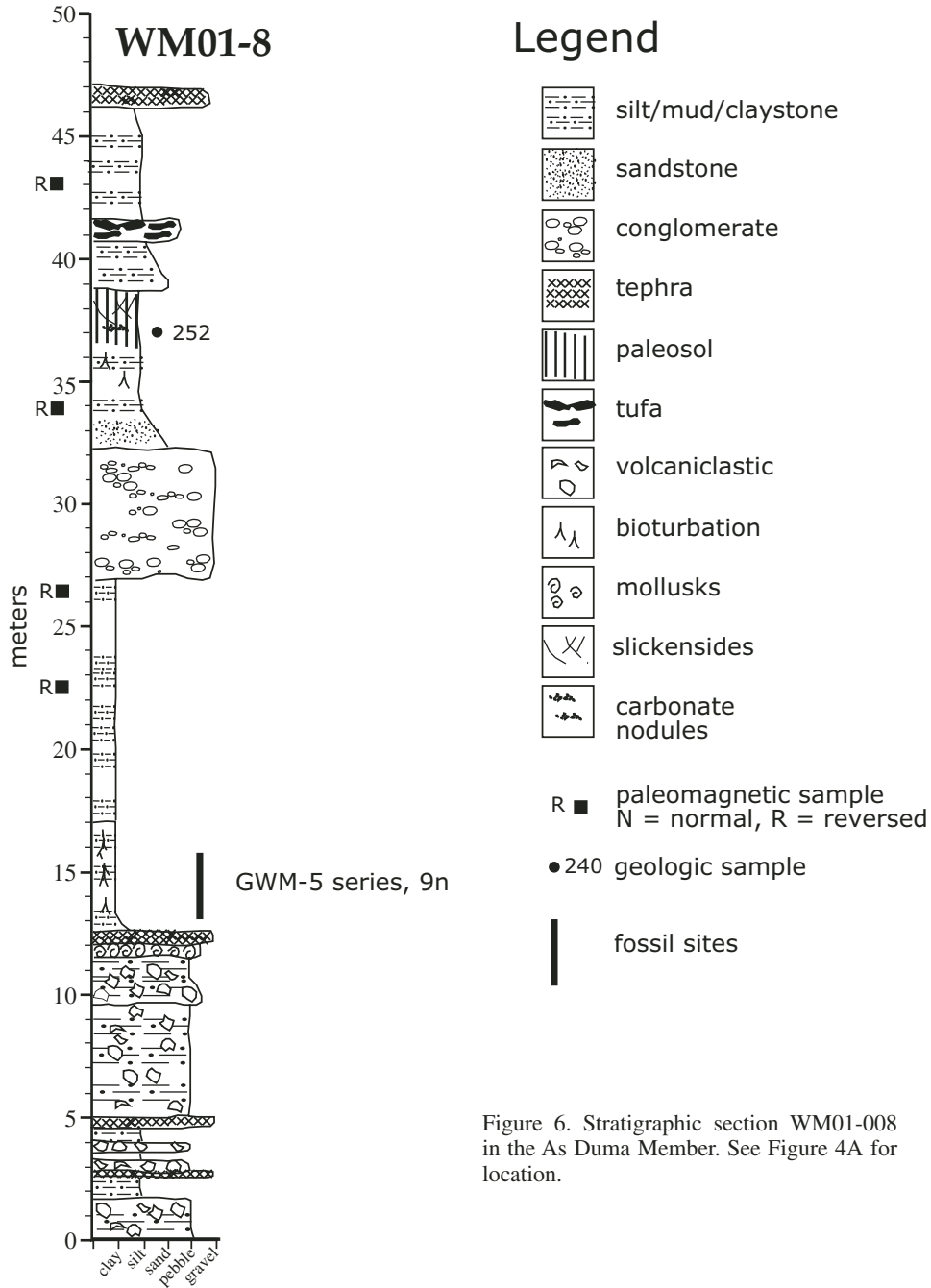


Figure 6. Stratigraphic section WM01-008 in the As Duma Member. See Figure 4A for location.

Most of the area is draped by younger gravels, but one badland area called As Aela by the local Afars exposes the continuous section that we present in Figure 8.

The section consists of interbedded siltstone, thin sands, gastropod-rich limestone, and a number of tephtras. Sedimentologically, it is much like the underlying Segala Noumou Member of the Sagantole Formation. Siltstone (Fl) is laminated, greenish, and contains fish remains over a 7–8-m-thick interval in the middle of the section (Fig. 8, shaded area). A gastropod-rich limestone can be traced out along the base of this interval,

which, combined with the fish fossil-rich siltstone, marks the transgression of a lake into the area. Above and below this interval, thin sandstone (Sr, St), conglomerate (Gm), and bedded (Fh) and massive (Fp) siltstone and mudstone characterize the section. We interpret all these latter lithologies as components of a small-scale alluvial system. The massive siltstones contain slickensides, subhorizontal cracks, and carbonate nodules, all features of modern Vertisols (Lynn and Williams, 1992).

The upper half of the As Aela section falls within the Basal and Sidi Hakoma Members of the Hadar Formation. A

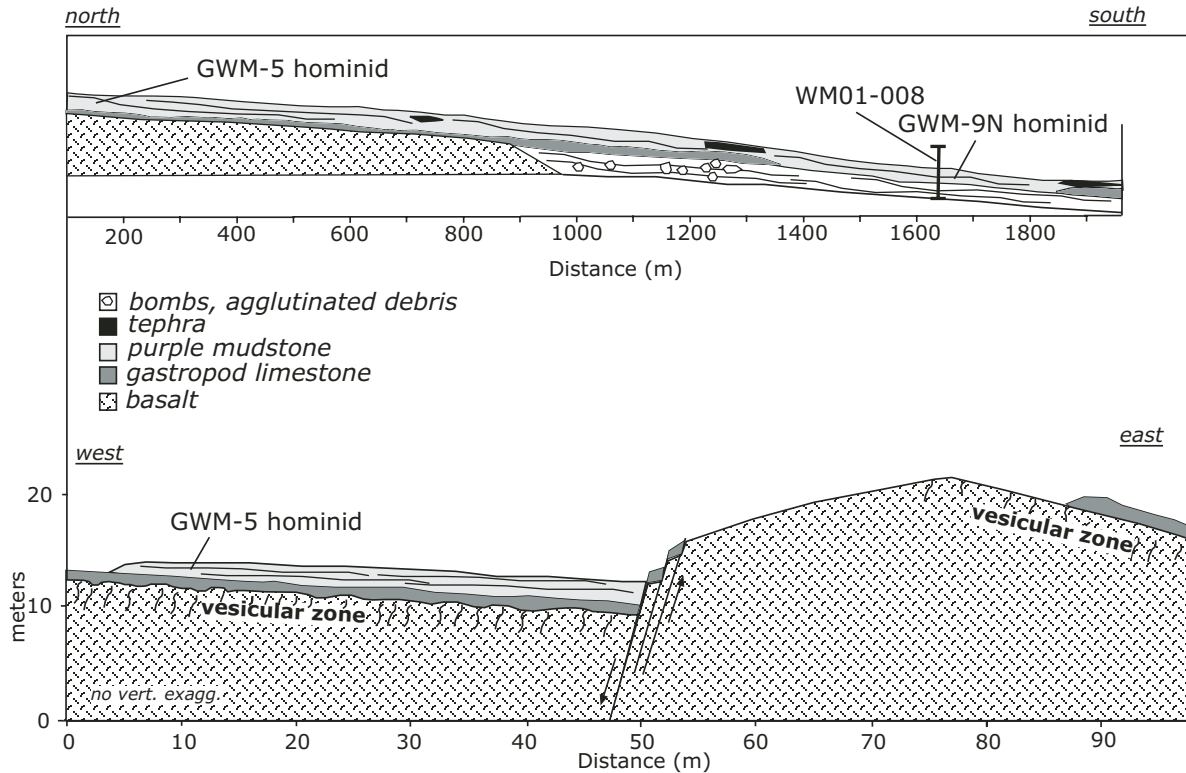


Figure 7. Detailed sections of fossil sites yielding *Ardipithecus ramidus* in the As Duma Member. See Figure 4A for locations and Figure 6 for legend.

conspicuous yellow pumice tephra (WMASH-65, Fig. 8) at the base of the exposed section at As Aela dates to 4.10 ± 0.07 Ma, whereas sanidine from a tephra (GONNL-68, Fig. 8) just below the top of the exposed section dates to 3.27 ± 0.10 Ma. In the type section of the Sagantole Formation in the Middle Awash Project area (see volume introduction), the top of the Sagantole Formation dates to 3.9 Ma. Wynn et al. (this volume) report on new findings from the Dikika area southeast of Gona where the base of the Basal Member of the Hadar Formation rests on a basalt and, near the base, contains the Ikini-Wargolo tephra (3.8 Ma). Glass is not preserved in tephtras at As Aela with which we could test for the presence of the Ikini-Wargolo tephra.

Busidima Formation

The term Busidima Formation is a recent redesignation (Quade et al., 2004) of the upper portion of the Hadar Formation, which was formerly referred to as the upper portion of the Kada Hadar Member (e.g., Aronson et al., 1996). Outcrops of the Busidima Formation cover almost all of the central and eastern portions of Gona and rest unconformably on the underlying Hadar Formation, which crops out only along the Awash River and Kada Gona (Fig. 9). In areas largely outside Gona, the contact between the Busidima and Hadar Formations is visible as an angular unconformity where the Hadar Formation was locally

faulted and tilted prior to deposition of the Busidima Formation (Wynn et al., this volume). The Busidima Formation at Gona is ~130 m thick and spans the period 2.7 Ma to <0.16 Ma.

In Quade et al. (2004), we described the stratigraphy and sedimentology of the Busidima Formation in some detail, as well as aspects of the geochronology. Since then, we have developed significant new information, especially for the upper half of the Busidima Formation. Our intent here is to expand upon the story presented in Quade et al. (2004), placing particular emphasis on the new stratigraphic and geochronologic data. This purpose is especially important for placing the abundant fossil hominid and archaeological remains in the Busidima Formation in a firm geochronologic framework. To achieve this, we measured a total of 56 stratigraphic sections in the Busidima Formation (Fig. 9), fully located and reproduced in Figures DR1 through DR9 (see footnote 1). From these sections, more generalized composite sections (Fig. 10) were constructed that summarize the key stratigraphic features and site locations in each area of Gona (Fig. 9).

Sedimentology and Stratigraphy

The Busidima Formation is composed of up to 130 m of sediment, but no more than ~50–70 m of thickness is measurable in any one area. Such thicknesses are visible in bluffs immediately along the Awash, where erosion has removed the upper half of the formation. The upper half of the formation is only preserved

TABLE 4. MAJOR-ELEMENT CHEMISTRY (UNNORMALIZED WT% OXIDE) OF TEPHRAS FROM GONA AND REGIONALLY

Sample no.	Tuff	Na ₂ O	F	Cl	K ₂ O	CaO	SiO ₂	Al ₂ O ₃	FeO	Fe ₂ O ₃	MgO	MnO	TiO ₂	Total	Age (Ma)
Busidima															
BUST-1	Boolihinan	1.71	0.18		3.12	0.24	73.78	9.82	4.79	5.32	0.02	0.17	0.33	94.33	1.60
BUST-2*	Dahuli	4.32	0.08		3.56	0.90	72.99	12.75	2.89	3.21	0.00	0.11	0.24	98.02	0.81
BUST-3	Dahuli	1.60	0.14		2.71	0.89	72.78	12.77	2.95	3.28	0.00	0.14	0.22	94.39	0.81
BUST-5	(=sub-Waterfall)	1.59	0.11		2.79	0.89	73.08	12.81	2.75	3.05	0.04	0.10	0.19	94.52	1.70
BUST-9	BBT	2.45	0.04		0.38	10.45	46.89	13.18	14.79	16.44	6.33	0.26	3.36	98.17	1.70
BUST-10*	Boolihinan	4.80	0.11		3.61	0.23	74.25	10.15	4.76	5.29	0.01	0.16	0.30	98.55	1.60
BUST-11	Dahuli	1.66	0.15		2.86	0.90	73.32	12.83	2.95	3.28	0.00	0.10	0.22	95.19	0.81
BSN-12 cr	Boolihinan	1.32	0.15		2.22	0.24	75.66	10.27	4.81	5.34	0.01	0.18	0.28	95.31	1.60
BUST-13	Dahuli	1.78	0.14		2.86	0.87	73.72	12.89	2.87	3.19	0.00	0.10	0.23	95.64	0.81
BUST-17	BBT	2.50	0.03		0.38	9.63	46.45	13.40	15.72	17.48	5.27	0.25	3.47	97.16	1.70
BUST-18	Below BSN-40	1.55	0.13		2.68	0.58	73.61	13.02	2.47	2.74	0.03	0.09	0.20	94.52	1.40
BUST-20	Silbo	1.40	0.11		2.16	0.14	77.82	10.78	3.22	3.58	0.03	0.16	0.19	96.15	0.75
BUST-21	Gawis	1.47	0.15		2.31	0.32	75.03	10.92	4.72	5.25	0.00	0.15	0.32	95.56	0.55
BUST-23*	Silbo	4.15	0.09	0.12	3.19	0.14	74.36	10.89	3.20	3.55	0.02	0.15	0.18	96.63	0.75
BUST-24*	Busidima	3.54	0.07	0.08	3.90	0.80	73.17	13.45	1.17	1.30	0.11	0.04	0.11	96.51	0.70
BUST-26*	Dahuli	4.17	0.06	0.10	3.52	0.85	71.85	12.88	2.95	3.28	0.00	0.06	0.23	96.86	0.81
BUST-27*	Dahuli	4.21	0.07	0.08	3.50	0.86	72.06	13.11	2.86	3.17	0.00	0.11	0.21	97.27	0.81
Asbole															
ASASH-1	Korina	2.04	0.10		3.20	0.81	74.66	13.03	2.21	2.45	0.01	0.08	0.14	96.39	0.1-0.2
ASASH-2	Odele	1.67	0.10		2.57	0.60	72.43	13.59	2.97	3.30	0.01	0.10	0.21	94.43	0.15
ASASH-3*	Waideo Vitric Tuff	2.06	0.12	0.188	3.69	0.23	75.52	9.80	5.13	5.70	0.01	0.28	0.33	97.43	0.16
ASASH-4	Talata	1.68	0.09		2.50	0.91	73.91	13.32	1.94	2.16	0.07	0.08	0.14	94.75	0.38
ASASH-5	Gawis	1.16	0.16		2.08	0.32	74.01	10.68	4.61	5.13	0.00	0.15	0.31	93.64	0.55
ASASH-6*	Bironita	5.41	0.10		3.50	0.54	70.95	11.64	5.48	6.09	0.01	0.25	0.40	98.48	0.60
ASASH-7	Gawis	1.57	0.13		2.71	0.32	73.44	10.82	4.58	5.09	0.01	0.14	0.31	94.20	0.55
ASASH-8*	Gawis	4.56	0.13	0.20	3.69	0.31	72.69	11.07	4.58	5.09	0.01	0.15	0.30	97.84	0.55
ASASH-10*	Gawis	4.08	0.10	0.20	3.31	0.32	73.54	11.16	4.63	5.15	0.01	0.13	0.34	97.97	0.55
ASASH-11*	Waideo Vitric Tuff	4.42	0.10	0.12	3.84	0.21	73.24	9.76	5.32	5.91	0.01	0.21	0.32	97.66	0.16
ASASH-12*	Waideo Vitric Tuff	4.44	0.13	0.12	3.89	0.22	74.10	9.65	5.34	5.93	0.00	0.22	0.32	98.54	0.16
ASASH-13*	Unnamed basaltic	3.06	0.04	0.03	0.69	8.99	47.17	13.81	14.71	16.35	5.21	0.24	3.81	97.77	0.15-0.25
ASASH-14*	Waideo Vitric Tuff	4.34	0.12	0.13	3.81	0.22	73.78	9.48	5.49	6.10	0.02	0.28	0.34	98.17	0.16
ASASH-15*	Unnamed	5.04	0.11	0.18	3.96	0.95	68.98	15.23	3.51	3.90	0.05	0.10	0.28	98.55	0.15-0.25
ASASH-16*	Korina	4.18	0.08	0.09	3.61	0.79	72.55	13.28	2.13	2.37	0.01	0.08	0.16	97.07	0.1-0.2
ASASH-17*	Talata	4.26	0.13	0.07	4.01	0.93	71.17	14.29	1.89	2.10	0.09	0.06	0.14	97.13	0.38
ASASH-18*	Waideo Vitric Tuff	4.49	0.09	0.12	3.83	0.21	74.12	10.22	5.27	5.85	0.01	0.20	0.32	98.99	0.16
ASASH-19*	Waideo Vitric Tuff	4.02	0.11	0.11	3.63	0.22	72.93	9.80	5.31	5.90	0.01	0.21	0.32	96.80	0.16
ASASH-20*	Unnamed	4.54	0.16	0.19	3.25	0.20	73.97	10.27	4.61	5.12	0.01	0.11	0.20	97.69	0.15-0.25
ASASH-21*	Waideo Vitric Tuff	4.60	0.15	0.12	3.90	0.22	73.75	10.01	5.34	5.94	0.01	0.21	0.31	98.75	0.16
ASASH-22*	Gawis	4.02	0.12	0.20	3.25	0.32	73.43	11.35	4.68	5.20	0.01	0.14	0.34	98.02	0.55
ASASH-23*	Gawis	1.83	0.14	0.20	3.00	0.32	74.67	11.12	4.69	5.21	0.03	0.14	0.33	96.62	0.55
ASASH-24*	Gawis	1.75	0.15	0.20	2.75	0.33	74.64	11.24	4.64	5.16	0.01	0.15	0.34	96.36	0.55
ASASH-25*	Unnamed	2.66	0.10	0.12	3.44	1.14	73.45	14.15	2.72	3.02	0.03	0.09	0.19	98.24	0.15-0.25
Kada and Ounda Gona															
AST-?*		3.69	0.05	0.11	3.27	0.34	72.77	12.23	2.69	2.99	0.00	0.09	0.18	95.58	?
AST-2		1.61	0.10		2.45	0.92	74.02	12.87	2.36	2.63	0.05	0.08	0.18	94.79	2.57
AST-2 (23)*		3.56	0.10		3.46	0.92	73.19	12.90	2.37	2.64	0.06	0.08	0.20	96.99	2.57
AST-3(24)		1.58	0.11		3.17	0.69	74.01	12.79	2.80	3.11	0.00	0.07	0.25	95.65	1.30
AST-3(85)		2.98	0.19		3.78	0.66	71.55	12.23	2.73	3.03	0.01	0.08	0.23	94.87	1.30
AST-3*		4.05	0.09		3.86	0.67	73.41	12.62	2.73	3.03	0.00	0.08	0.24	97.94	1.30

(continued)

TABLE 4. MAJOR-ELEMENT CHEMISTRY (UNNORMALIZED WT% OXIDE) OF TEPHRAS FROM GONA AND REGIONALLY (continued)

Sample no.	Tuff	Na ₂ O	F	Cl	K ₂ O	CaO	SiO ₂	Al ₂ O ₃	FeO	Fe ₂ O ₃	MgO	MnO	TiO ₂	Total	Age (Ma)
Kada and Ounda Gona (continued)															
Gonash-15*	Fialu(= AST-3 ?)	4.35	0.08		3.40	0.65	73.08	13.03	2.47	2.75	0.05	0.10	0.21	97.58	1.30
Gonash-18	Fialu(= AST-3 ?)	1.79	0.12		3.21	0.69	73.33	13.37	2.64	2.94	0.05	0.08	0.20	95.63	1.30
Gonash-20	Fialu(= AST-3 ?)	1.89	0.14		3.21	0.74	73.19	13.44	2.70	3.00	0.07	0.09	0.21	95.84	1.30
Gonash-24*	Fialu(= AST-3 ?)	2.38	0.13	0.122	3.41	0.69	73.85	13.74	2.62	2.92	0.05	0.09	0.20	97.45	1.30
Gonash-24	Fialu(= AST-3 ?)	2.73	0.18		3.32	0.66	72.27	12.91	2.23	2.48	0.07	0.08	0.20	95.00	1.30
Gonash-25*	Unnamed	3.71	0.11		2.96	0.18	75.92	10.59	3.26	3.62	0.01	0.13	0.23	97.25	?
Gonash-30	Camp	1.51	0.07		2.54	0.77	74.25	13.69	1.95	2.16	0.16	0.06	0.25	95.39	1.00
Gonash-31	Camp	1.52	0.09		2.82	0.78	72.85	13.71	1.92	2.14	0.17	0.06	0.24	94.27	1.00
Gonash-32*	Ridge	3.61	0.08		2.65	0.59	72.55	13.60	3.37	3.75	0.03	0.13	0.29	94.04	0.90
Gonash-33*	Camp	4.24	0.08		4.22	0.80	72.74	13.65	1.89	2.10	0.16	0.05	0.24	98.18	0.95
Gonash-37	Butte	2.26	0.08		3.15	0.18	73.97	8.99	5.45	6.06	0.10	0.28	0.37	95.02	<0.10
Gonash-40	Butte	0.46	0.06		1.33	0.21	74.23	9.17	5.22	5.81	0.02	0.03	0.04	95.02	<0.10
Gonash-43	Ala Kata	1.90	0.10		2.79	0.20	76.34	11.31	3.07	3.42	0.00	0.11	0.17	96.15	0.80
Gonash-44	Camp	1.75	0.07		3.52	0.81	73.81	13.96	1.97	2.20	0.17	0.05	0.25	96.49	0.95
Gonash-47	Sub-Fialu A	0.85	0.15		1.10	0.43	73.81	10.46	7.23	8.03	0.04	0.31	0.47	95.00	1.40
Gonash-48*	Sub-Waterfall	3.08	0.08		2.89	0.88	71.95	12.88	2.63	2.92	0.04	0.09	0.22	94.88	1.70
Gonash-49*	Waterfall	2.32	0.12		1.99	0.21	74.27	9.31	5.16	5.74	0.01	0.18	0.30	94.04	1.70
Gonash-61	Ala Kata	1.43	0.15		2.27	0.19	73.84	11.09	3.06	3.41	0.00	0.10	0.18	92.45	0.80
Gonash-62	Sub-Waterfall	1.61	0.11		2.55	0.90	72.85	13.28	2.61	2.90	0.03	0.09	0.22	94.38	1.70
Gonash-68	Fialu(=AST-3)	2.01	0.10		2.61	0.77	73.05	13.78	2.75	3.05	0.07	0.09	0.21	95.61	1.30
Gonash 68*	Fialu(=AST-3)	1.92	0.11	0.121	2.62	0.71	73.42	13.42	2.61	2.68	0.02	0.09	0.18	94.10	1.641 ± 0.028
Gonash-73	Sub-OGS-12	1.43	0.12		2.58	0.71	74.02	12.40	2.41	2.68	0.02	0.09	0.18	94.10	1.50
Gonash-76*	Sub-Fialu B	3.39	0.08	0.06	3.23	1.05	70.98	12.87	3.00	3.33	0.04	0.10	0.27	95.19	1.50
Gonash-77*	Sub-Fialu C	3.57	0.06		3.81	0.97	69.96	12.76	2.75	3.06	0.03	0.09	0.26	94.47	1.50
Gonash-78*	Calicified Fialu	4.47	0.12	0.12	3.59	0.77	71.34	14.01	2.72	3.02	0.07	0.10	0.25	97.69	1.30
Gonash-80*	Sub-Fialu D	1.55	0.09	0.05	2.12	1.30	70.03	13.35	3.67	4.08	0.45	0.10	0.53	93.43	1.40
Gonash-82*	Camp	2.30	0.11	0.12	3.45	0.77	69.01	13.89	1.89	2.10	0.16	0.04	0.25	92.06	1.00
Gonash-83*	Ridge Tuff	1.63	0.10	0.09	2.77	0.72	71.14	12.87	3.21	3.57	0.01	0.13	0.24	93.14	0.90
Gonash-84*	Alakata	2.17	0.13	0.14	3.07	0.20	75.90	11.52	3.05	3.39	0.01	0.11	0.18	96.63	0.80
Gonash-85*	Unnamed	1.76	0.10	0.09	2.41	0.86	73.75	12.93	2.87	3.19	0.00	0.11	0.24	95.32	0.70
Gonash-86*	Ken-Di	2.67	0.08	0.13	1.49	0.28	71.07	9.44	6.43	7.15	0.22	0.28	0.33	92.40	0.50
Gonash-87*	Below Ken-Di	4.58	0.14	0.16	2.93	0.14	74.06	10.17	3.58	3.98	0.07	0.27	0.32	96.52	0.70
Dana Aoule															
Danash-11		1.25	0.16		2.04	0.34	74.65	12.42	2.71	3.02	0.00	0.08	0.18	94.00	?
Western Margin															
WM-4*		0.581	0.05	0.10	1.28	0.17	73.92	10.07	3.74	4.15	0.19	0.19	0.28	90.57	?
Extraregional tuffs correlated to Gona (data source)															
Unnamed (1)	DSDP-DEM-4-1	3.77	0.49		4.09	0.25	72.82	9.92	4.82	5.35	0.00	0.15	0.22	97.45	1.63
Silbo (2)	(Turkana)	3.13			3.79	0.15	74.19	10.54	3.17	3.52	0.02	0.15	0.18	95.83	0.75
Silbo (2)	(Gadeb)	3.73			4.59	0.15	74.4	10.54	3.23	3.59	0.03	0.15	0.2	97.55	0.75
Bironita (3)	E02-1111	3.87			3.29	0.61	72.48	12.69	5.79	6.44	0.02	0.22	0.38	100	0.64 ± 0.03
Bironita (3)	E02-1126	5.08			3.62	0.57	71.57	12.02	5.78	6.42	0.02	0.25	0.45	100	0.64 ± 0.03
Bironita (3)	E02-1127	4.38			3.79	0.59	71.77	12.52	5.72	6.36	0.02	0.22	0.36	100	0.64 ± 0.03
Bironita (3)	E02-1151				2.97	0.58	73.89	12.88	5.37	5.97	0.02	0.25	0.37	100	0.64 ± 0.03
Waideo Vitric (4)	MA92-01 (middle Awash)	3.63			3.39	0.24	70.1	9.32	6.27	6.27	0	0.2	0.34	93.48	0.16
Waideo Vitric (4)	Unnamed (Konso)	4.11			4.11	0.26	69.84	9.23	5.7	5.7	0	0.2	0.33	92.82	0.16

Note: References: (1) Peter DelMenocal (2004, personal commun.); (2) Haileab (1994); (3) Clark et al. (1994); Geraards et al. (2004); (4) Clark et al. (2003).

*Run at 10 microns, 8 nA, 15 kV for alkalis; all other Gona analyses at 2 microns, 20 nA, 15 kV. Average of 20 shards per sample for Gona analyses.

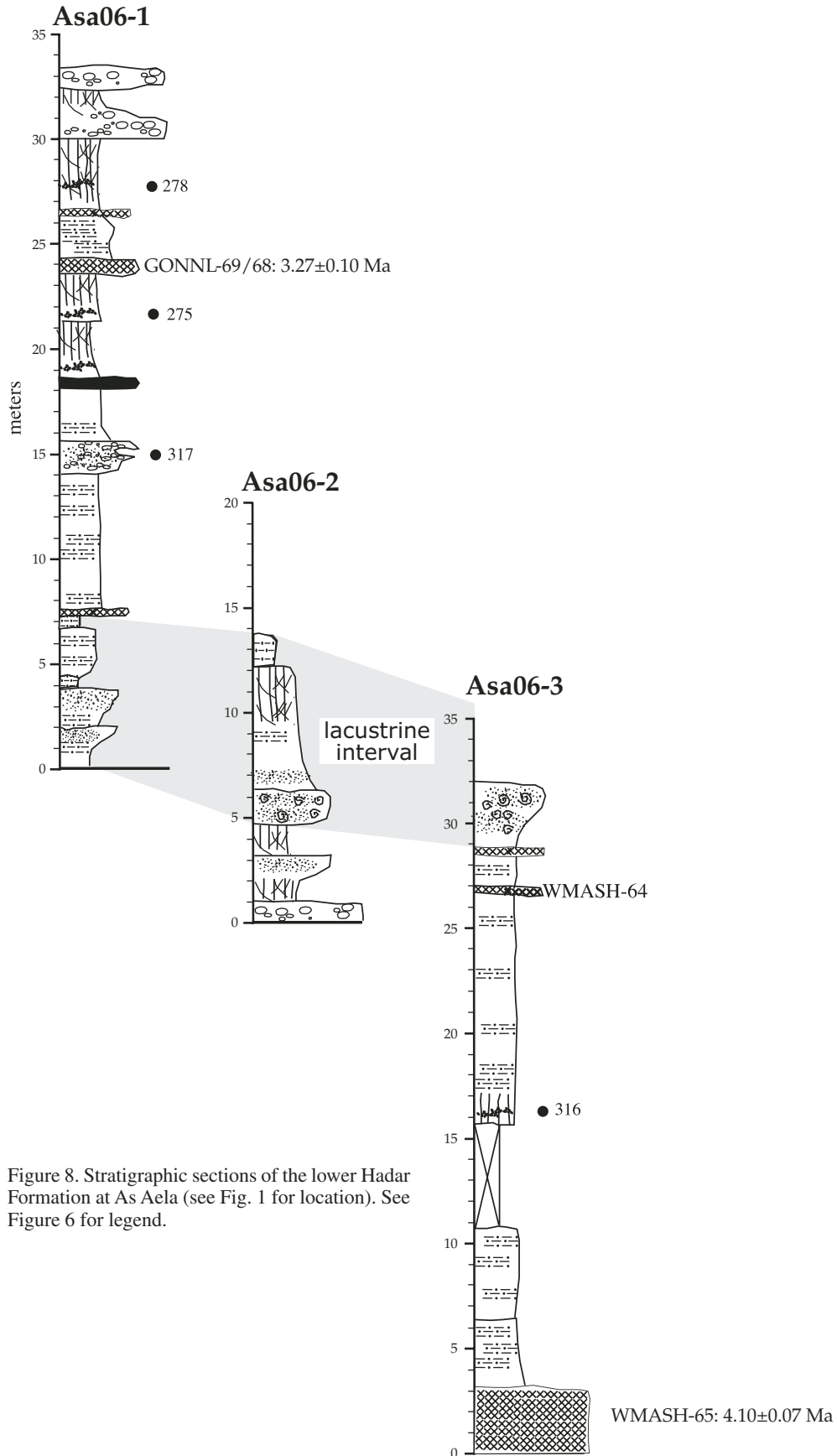


Figure 8. Stratigraphic sections of the lower Hadar Formation at As Aela (see Fig. 1 for location). See Figure 6 for legend.

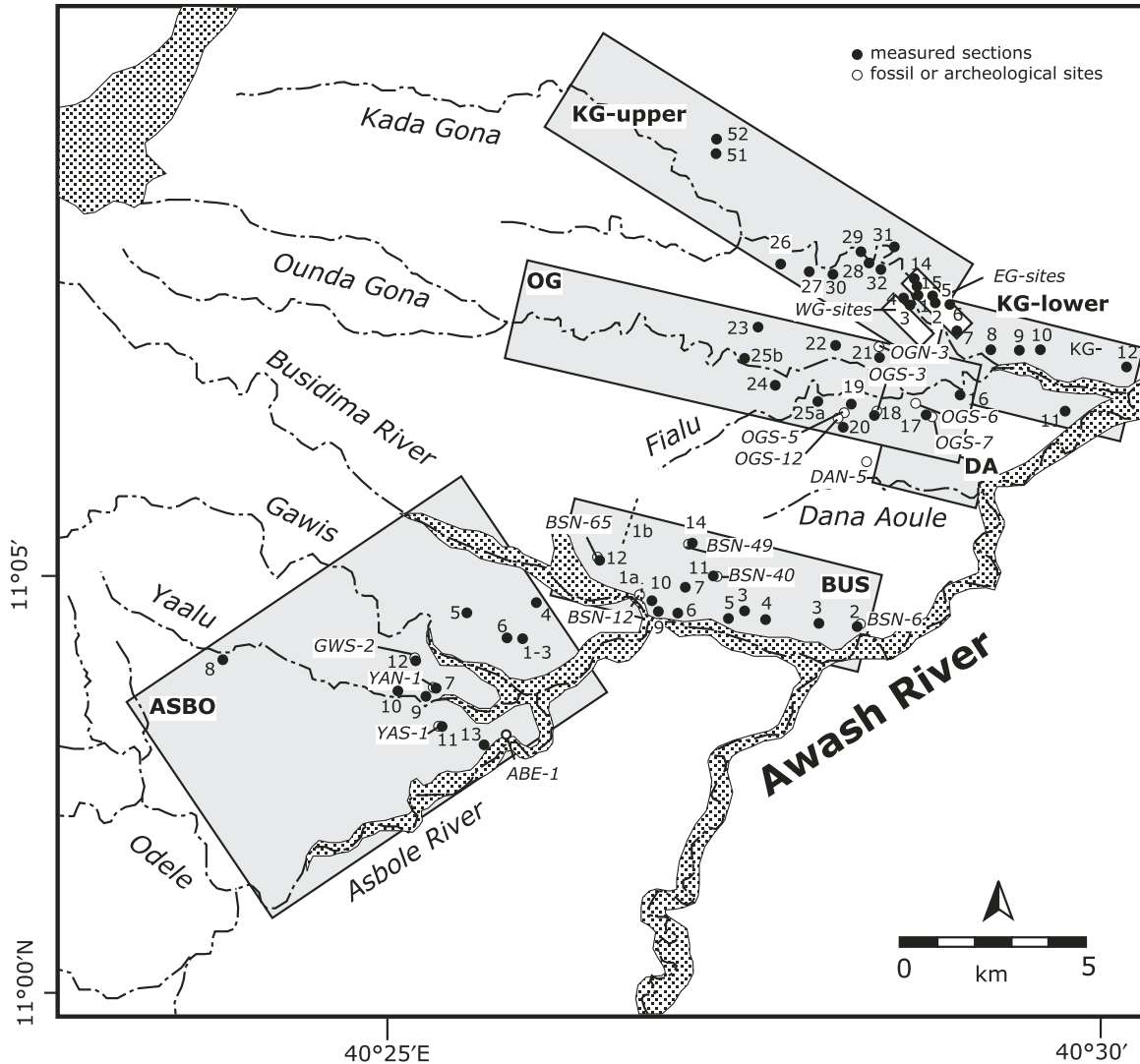


Figure 9. Location of key fossil and archaeological localities (open circles) and measured sections (filled circles) in the Busidima Formation. Individual sections are prefixed by area as follows in figure and in Figures DR1–DR9 (see text footnote 1): ASBO—Asbole area, KG—Kada Gona, OG—Ounda Gona, BUS—Busidima, and DA—Dana Aoule. Composite stratigraphic sections for each of these areas are presented in Figure 10.

in the headwaters of the Asbole, Busidima, Ounda, and Kada Gona drainages, far removed to the west of the Awash (Fig. 1). The Busidima Formation thins eastward into the Dikika Project Area as it approaches the hinge of the modern Awash half-graben (Wynn et al., this volume).

The base of the Busidima Formation in the Gona Paleoenvironmental Research Project area is marked by a major unconformity cut into fluvial and lacustrine sediments of the underlying Hadar Formation (Figs. 3E and 3F). Above the unconformity, the Busidima Formation contains 1–3-m-thick conglomerates, in sharp contrast to the dominance of sand and mudstone in the underlying Hadar Formation. This makes the basal contact of the Busidima Formation easy to recognize and map at Gona (Fig. 1).

The Busidima Formation consists entirely of weakly consolidated sediments interlayered with very dispersed air-fall tephras (Quade et al., 2004). Lithologies include massive (Gm) to trough (Gt) cross-bedded conglomerate, rippled (Sr), trough cross-bedded (St), and massive (Sm) sandstone, and bedded/laminated (Fh/FI) to massive (Fp) mudstone. In the lower half of the Busidima Formation, this succession of lithologies is organized in very regular 6–23-m-thick packages, fining upward from conglomerate at the base of each package to massive mudstones at the top. Quade et al. (2004) interpreted these fining-upward packages to represent deposition by a coarse-grained, meandering, ancestral Awash River. This contrasts with previous interpretation of these features of Yemane (1997), who viewed them as representing deposition on alluvial

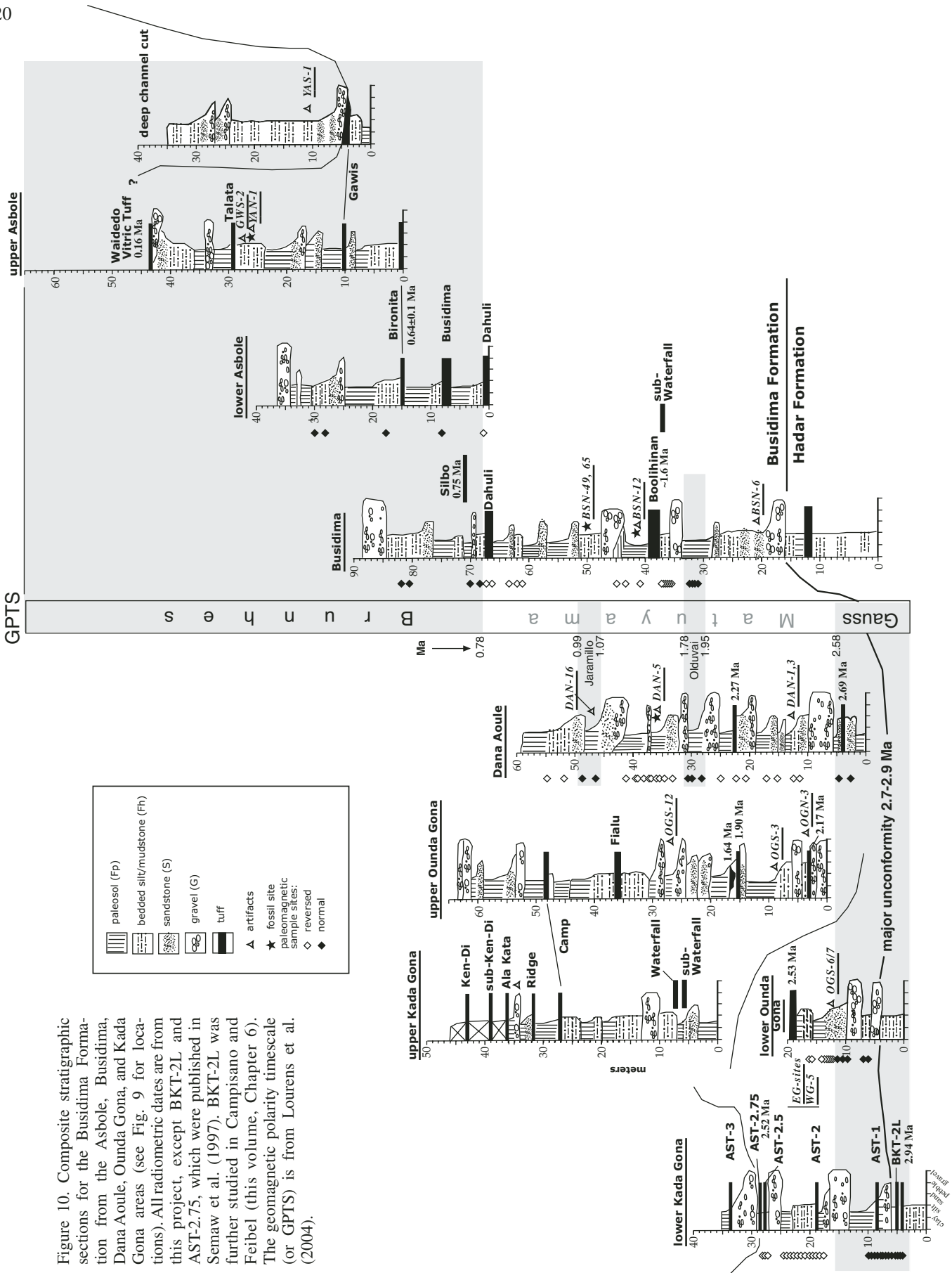


Figure 10. Composite stratigraphic sections for the Busidima Formation from the Asbole, Busidima, Dana Aoule, Ounda Gona, and Kada Gona areas (see Fig. 9 for locations). All radiometric dates are from this project, except BKT-2L and AST-2.75, which were published in Semaw et al. (1997). BKT-2L was further studied in Campisano and Feibel (this volume, Chapter 6). The geomagnetic polarity timescale (or GPTS) is from Lourens et al. (2004).

fans on the valley margins (rather than along its axis) by sheet-flooding. The evidence in favor of deposition by the ancestral Awash along the valley axis—rather than by its valley-flanking tributaries—is: (1) paleocurrent directions are N-NW, parallel to the flow of the modern Awash River at Gona today, (2) heterolithic gravels (“Type I” lithofacies gravels) in Busidima Formation are identical to those carried by the modern, coarse meandering Awash River, and (3) the fining-upward packages of the Busidima Formation contain clear fossil evidence (crocodiles, hippopotamus, marsh cane rats) of perennial water flow, much like the modern Awash, and unlike its modern tributaries, which are nearly all ephemeral (Quade et al., 2004).

We carefully mapped out the number and distribution of type I lithofacies gravels associated with the ancestral Awash River along a 1.5 km reach of the Busidima River (Fig. 1) in order to understand its long-term behavior. Eight separate conglomerates in fining-upward packages were identified (Figs. DR5–DR7 [see footnote 1]), with an average thickness of 16 ± 5 m. The conglomerates are most numerous toward the east, in the area of the present position of the Awash River. Westward, the gravels feather out, disappearing near the confluence of the Busidima and Asbole Rivers. The gravels are distributed from the base of the formation (2.7 Ma) up to just below the Dahuli Tuff (0.81 Ma). This suggests a return time of the ancestral Awash River across Gona of eight conglomerates per 2 m.y., or once every $\sim 250,000$ yr.

Another important observation from the Busidima Formation is the presence of two distinct types of alluvial lithofacies: the type I lithofacies, containing the distinctive coarse gravels just described and associated with the ancestral Awash River, and type II lithofacies gravels, consisting of finer and less mature clasts in generally thinner conglomerate bodies than in type I (Quade et al., 2004). The type II lithofacies are interpreted to represent deposition by eastward-flowing paleotributaries to the ancestral Awash, tributaries that were in most, but not all, cases ephemeral.

The character of the Busidima Formation changes between 1.0 and 1.5 Ma, between the Dahuli Tuff (0.81 Ma) (Quade et al., 2004) and Boolihinan (1.6 Ma) Tuff. At about this level, the type I lithofacies gravels disappear (gravel 4.3, Fig. DR7 [see footnote 1]). After ca. 1.0 Ma, much finer sediments dominate, mostly thick paleosols (Fp) and their accompanying minor type II lithofacies gravels and sands (Fig. 3G). The density of mammalian fossils remains also drops off, an indication that the ancestral Awash River had moved eastward out of the Gona area. These gave way to a distal alluvial-fan setting characterized by broad surfaces that experienced deep pedogenesis, interspersed with small, largely ephemeral paleochannels filled by type II lithofacies.

Our surveys of the Asbole area (Fig. 1) since 2004 reveal that thick conglomerate bodies (type I) with coarse, well-rounded clasts reappear in the upper part of Busidima Formation (Fig. 3H). This transition occurs above the Bironita (0.64 ± 0.03 Ma) but below the Gawis (0.5 Ma) tephtras. At least two

very thick (17–30 m) fining-upward cycles are represented. The younger cycle contains abundant well-preserved aquatic mollusks, clearly attesting to perennial river flow.

Age Constraints

A rich variety of geochronologic constraints is available from the Busidima Formation, including over 35 tephtras. Seven of these have been dated using $^{40}\text{Ar}/^{39}\text{Ar}$ (Table 1), all in the lower half of the Busidima Formation. Most tephtras are aphyric but preserve fresh glass available for major-element analysis and hence potential tephrostratigraphic correlation. Some of these tephtras can be confidently correlated with well-dated regional ash-fall events. The abundant well-bedded siltstone in the Busidima Formation yields robust magnetic polarities, providing key constraints on the age of the Busidima Formation and its rich archaeological and paleontological archive.

Tephtra Occurrences

In the field, most of the tephtras are either light gray or white. The white color nearly always denotes partial to complete alteration of glass to clay, whereas the gray color seems to be the primary color of unaltered glass, except where basaltic. Altered tephtras are restricted in both time and space. The altered tephtras are confined entirely to the lower half of the Busidima Formation (older than 1.6 Ma). Below this level, glass in most tephtras shows some degree of alteration and, in some cases, complete conversion to secondary clays. The altered tephtras are closely associated with the type I lithofacies of the paleo-Awash River, suggesting a causal connection. In this setting, the tephtras would have been saturated shortly after burial by shallow groundwater on the ancestral Awash floodplain, probably leading to their alteration. By contrast, tephtras in the levels from 0.5 to 1.5 Ma at Gona fell largely on distal alluvial fans and may have remained dry or only seasonally wetted even after burial due to the deep levels of the water table. As noted previously, the ancestral Awash River returned to Gona ca. 0.5 Ma, which would have placed almost all tephtras at Gona in the saturated zone. However, such conditions may have been brief enough (<0.3 m.y.) for the glass in the tephtras to be largely preserved.

Tephtra occurrence is laterally very discontinuous in the Busidima Formation at Gona, in sharp contrast to the Hadar Formation, where tephtras are readily traceable across long distances and between project areas (Roman et al., this volume; Wynn et al., this volume; Campisano et al., this volume, Chapter 6). For example, the Boolihinan and Dahuli Tuffs are major stratigraphic markers in the Busidima area, but they have not been found, despite intensive searching, along the Ounda Gona, Kada Gona, or Dana Aoule drainages. Conversely, the Fialu and Camp Tuffs are conspicuous and continuous over broad areas of Ounda and Kada Gona, and yet they have not been found along the Busidima. This pattern is an artifact of the cut-and-fill nature of the stratigraphy of the Busidima Formation by the paleo-Awash River. In many areas, this incision and backfilling by younger channels into older deposits are quite visible. For example, the channel containing

site OGS-3 along the lower Ounda Gona (Fig. 10) is readily mappable and involves ~14 m of incision. The channel inset containing YAS-1 along the upper Asbole, involving at least 35 m of incision followed by backfilling, is another example (Fig. 10).

⁴⁰Ar/³⁹Ar Dates

Seven ⁴⁰Ar/³⁹Ar dates are available from the Busidima Formation, all from the lower portion (Table 1). All the dates are on sanidine or plagioclase. They range from 2.69 ± 0.06 Ma to 1.641 ± 0.028 Ma.

Magnetostratigraphy

Paleomagnetic analyses are available from Semaw et al. (1997) and Semaw et al. (2003) for short intervals at the base of the Busidima Formation, and from data published here for the rest of the formation (Table DR1 [see footnote 1]). Over 100 sites are involved, and three to four samples were analyzed per site. Together, the data greatly refine our previous knowledge of the geochronology of the Busidima Formation.

Nearly all the major magnetic polarity intervals covering the last 2.7 m.y. appear to be represented at Gona, dated using the geomagnetic polarity timescale (GPTS) of Lourens et al. (2004). Our results show that sediments at the base of the Busidima Formation from Kada Gona (Semaw et al., 1997), at Ounda Gona (Semaw et al., 2003), and at Dana Aoule (Fig. 10) display normal polarity and belong to the Gauss chron. The Gauss-Matuyama transition (2.58 Ma) is very well fixed and occurs ~9 m below tephra AST-2.75 (2.517 ± 0.15) along the Kada Gona, 8 m below tephra GONASH-14 (2.534 ± 0.30) at Ounda Gona, and less than 5 m above tephra GONASH-39 (2.69 ± 0.06) at Dana Aoule (Figs. 3F and 10). Above these stratigraphic levels, only the Dana Aoule, Busidima, and lower Asbole areas have been sampled in detail. The Olduvai chron (1.78–1.95 Ma) has been detected at both Dana Aoule and Busidima, providing vital local geochronologic constraints on hominid remains and archaeological sites in those areas. The very short Jaramillo chron (0.99–1.07 Ma) only has been identified near the top of the Dana Aoule section (Fig. 10). The Brunhes-Matuyama (BM) boundary (0.78 Ma) occurs slightly (<1 m) above the Dahuli Tuff along the Busidima and the lower Asbole (Fig. 10). This is confirmed by the presence of the Silbo (0.75 Ma) and the Bironita (ca. 0.64 ± 0.03 Ma) Tuffs 4.5 and 15 m, respectively, above the Brunhes-Matuyama boundary (see next section).

Tephrostratigraphy

Mapping and major-element analyses reveal more than 35 chemically distinct tephras at Gona (Table 4). The distinctions are based on visual inspection of the glass morphology, on compositional distinctions (mainly CaO, FeO, TiO₂, followed by Al₂O₃, SiO₂, MgO, and MnO), and on stratigraphic level. All these criteria are important, because, in some cases, glass composition can be very similar (Fig. 11; Roman et al., this volume), but the tephras are clearly different based on stratigraphic position. Reliable analyses of alkalis were obtained for about two-thirds of the tephras

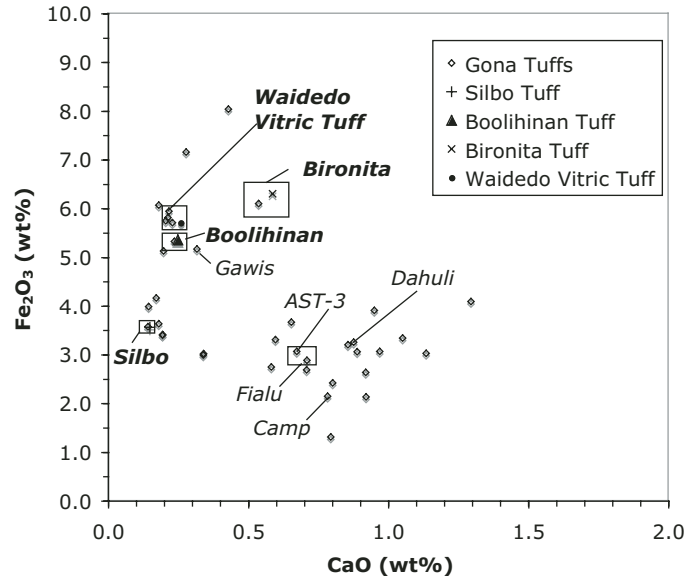


Figure 11. Plot of CaO versus Fe₂O₃ (wt% oxides) for all tephras (open diamonds) at Gona. The plots of some major tephra markers at Gona are noted, and the four Gona tephras with their regional tephra correlations are indicated in boxes.

at Gona, allowing us to classify them chemically. Aside from two basaltic tephras (Table 4; BUSTASH 9/17 and ASASH-13), all other glass in tephras at Gona are rhyolitic and subalkaline (Roman et al., this volume).

Nearly all the tephras analyzed from the Busidima Formation are tied to measured stratigraphic sections, thus placing them in a firm local stratigraphic context. A combination of field evidence, radiometric and magnetostratigraphic dating, and extra-regional correlations allows us to place many of the tephras in an absolute chronologic framework (Fig. 10). Tephras with multiple occurrences and widespread distribution at Gona include: the sub-Waterfall (ca. 1.7 Ma), Boolihinan (1.6 Ma), AST-3/Fialu (~1.3 Ma), Camp (ca. 1.0 Ma), Dahuli (0.81 Ma), Silbo (0.75 Ma), Bironita (0.64 Ma), Gawis (ca. 0.55 Ma), Talata (ca. 0.38 Ma), and Waidedo Vitric (or WAVT) (0.16 Ma) Tuffs. More restricted in outcrop but stratigraphically important tephras include the Ridge (ca. 0.9 Ma), sub-Fialu A, B, C, and D (1.4–1.5 Ma), and Butte (<0.1 Ma?) Tuffs.

At least eight tephras can be correlated to tephras outside Gona, based on their major-element composition (Fig. 11 for CaO versus Fe₂O₃) and stratigraphic position. These include the Boolihinan, Silbo, Bironita, Dahuli, Ken-Di, Korina, Odele, and Waidedo Vitric Tuffs. The Boolihinan Tuff (Table 4: BUST-1, -10, BSN-12cr) is chemically very close to Deep Sea Drilling Project (DSDP) DEM-4-1 tephra at Ocean Drilling Program (ODP) Site 722 from the Gulf of Aden, dated at 1.6 Ma (Table 4; P. deMenocal et al., 2003, personal commun.). This correlation is supported by the position of the Boolihinan ~5 m above the top (1.78 Ma) of the Olduvai chron. The Dahuli Tuff, present but undated at Hadar (Yemane, 1997; Campisano et al., this volume,

Chapter 6), is found at Gona just below the Brunhes-Matuyama boundary; as such, we estimate its age to be 0.81 Ma. We correlate samples BUST-20 and -23 (Table 4) with the Silbo Tuff (0.75 Ma), another major tephra that fell over broad areas of East Africa and the Arabian Sea (McDougall, 1985; Haileab and Brown, 1994). This is consistent with its position ~5 m above the Brunhes-Matuyama (0.78 Ma) boundary. Sample ASASH-6 (Table 4) can be confidently correlated with the Bironita Tuff (ca. 0.64 ± 0.03 Ma; Clark et al., 1994 for the Middle Awash Project; Geraads et al., 2004, for the Dikika Project), at 14 m above the Brunhes-Matuyama boundary. The Ken-Di Tuff was found just south of the drainage divide separating the Gona and Hadar project areas and at the top of our measured section in that area. With the distinctively high %Fe₂O₃ of its main glass mode, the Ken-Di is also reported from the upper Busidima Formation at Hadar (Campisano et al., this volume, Chapter 6) and Dikika (Wynn et al., this volume). Two minor tuffs, the Korina and the Odele, are found in the uppermost Busidima Formation at both Gona and Dikika (Roman et al., this volume). Finally, a very prominent and continuous tephra sampled at six locations (Table 4) yields an excellent chemical match to the Waidedo Vitric Tephra (0.16 Ma; Clark et al., 2003) from the nearby Middle Awash Project area, consistent with its position very near the top of the section at Gona.

Archaeological Sites

The Busidima Formation contains almost the entire known (2.7 to <0.16 Ma) record of stone tool-making, arguably the longest documented archaeological record in one location in the world. Archaeological sites containing artifacts typical of the oldest recognized stone tool-making tradition, the Oldowan Industrial Complex, are numerous in the lowest stratigraphic levels at Gona (Semaw et al., 1997). They range in age from 2.5 to 2.6 Ma for the oldest sites (OGS-6/7, BSN-6, and the EG series sites) and 2.2–1.9 Ma (OGS-3, OGN-3, WG-5) for the youngest sites (Fig. 9; Table 2). As described in Quade et al. (2004), the tools are found in the sandy to silty, middle to upper portions of the fining-upward sequences so typical of the lower Busidima Formation. Moreover, gravels of the type I lithofacies lie at the base of these fining-upward sequences at all the known Oldowan sites. The sedimentologic evidence therefore consistently points to a floodplain setting for these sites adjacent to the channel of the ancestral Awash River. OGS-7 (Fig. 3F) is one such example, where dense concentrations of lithic debris occur on a sand lens marginal to a type I gravel (Semaw et al., 2003). These types of gravels are found largely in point bars of the modern Awash River. Aphanitic clasts from such point bars in the paleo-Awash River were carefully selected for by early hominids in Oldowan tool manufacture (Stout et al., 2005).

Archaeological sites containing implements belonging to the Acheulian Industrial Complex are also common at Gona, sometimes with associated hominid remains. The oldest sites (1.6–1.3 Ma) are represented by BSN-12, BSN-49, and BSN-65, OGS-12, and OGS-5. Younger examples of Acheulian sites

include DAN-16 (1.0 Ma), ABE-1 (0.6 Ma), and GWS-2 (0.4 Ma) for the terminal Acheulian. As with the Oldowan sites, all these sites are found in the middle and upper portions of fining-upward sequences, indicative of a floodplain setting (Fig. 3G, BSN-49). Unlike the Oldowan sites, several important Acheulian sites, such as OGS-5, -12, BSN-49, and several sites at the YAN-1 stratigraphic level, are found in association with the type II lithofacies, a pattern seen elsewhere in East Africa (Rogers et al., 1994). Fossil evidence (aquatic snails, *Thryonomis swinderiansis* or marsh cane rat) suggests that these archaeological sites were located on large perennial tributaries to the ancestral Awash River.

Late Stone Age (?) sites such as YAS-1 in the upper part of the section are found in association with a deep (35 m) paleo-channel filled with the type I lithofacies along the upper Asbole (Fig. 10). The detailed context of these youngest archaeological sites is work in progress.

REGIONAL GEOLOGICAL SYNTHESIS AND HOMINID PALEOENVIRONMENTS

The history of basin filling over the past ~6.4 m.y. at Gona is nearly continuously represented by volcanic but mainly sedimentary deposits (Fig. 12). In most respects, the geologic history of that basin filling at Gona follows the classic tectono-sedimentary evolution of rift basins described by a number of studies (Lambiase, 1990; Gawthorpe and Leeder, 2000). In this progression, basins gradually expand, deepen, and interconnect, producing a very distinctive sedimentary succession. The basic structure of continental rifts is the half-graben (Bosworth, 1985); this is arguably the basin setting for Gona and surrounding project areas over the past 6.4 m.y., based on two general lines of evidence: The first is the increase in the eastward dip of beds in the Adu-Asa (5–20°E) through to the Sagantole (mostly 5–10°E) and Hadar Formations (1–5°E), which strongly suggests progressive rotation along a common normal fault or set of faults located on the east side of the area. This kind of “fanning” of dips is typical of half-graben growth structures in rifts (Schlische, 1991). The second is the eastward thickening of deposits in Hadar Formation (Dupont-Nivet et al., this volume; Wynn et al., this volume). This is presumed to occur in the direction of the hanging-wall depocenter of a half-graben downdipping to the east. By contrast, the Busidima Formation dips and thickens westward (Wynn et al., this volume), pointing to a change in the polarity of the half-graben, as the basin-bounding As Duma fault activated ca. 2.9 Ma.

Broadly speaking, there are four distinct phases represented at Gona that contrast in lithology, sediment accumulation rates, and depositional environment (Fig. 12). These include the “fault initiation” stage (after Gawthorpe and Leeder, 2000), represented by the Adu-Asa Formation (>6.4–5.2 Ma) in which basaltic volcanic rocks dominate over sediments in an incipient extensional basin. The second “interaction and linkage stage” is represented by the Sagantole (4.6–3.9) and Hadar (3.8–2.9) Formations. Here, local igneous activity decreased and finally disappeared except

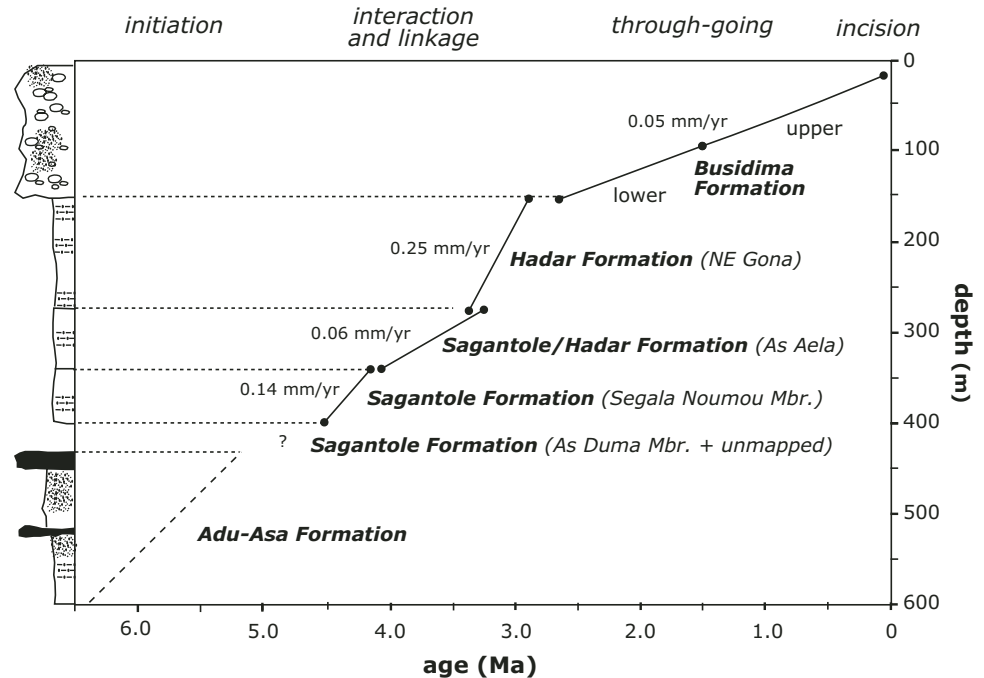


Figure 12. Sediment accumulation history and rates (in mm/yr) for the formations represented at Gona and the major tectonic stages (after Gawthorpe and Leeder, 2000).

along the As Duma fault, the basin enlarged and deepened, and sedimentation rates were very high (Fig. 12). Flow through the basin was likely partially confined at some downstream point north of Ledi-Geraru, impounding sediments and producing lakes and low-gradient rivers. The third “through-going fault stage” is represented by the Busidima Formation (2.7 to <0.2 Ma), when local depocenters were linked into a continuous drainage system by a single, large-scale meandering river. At the same time, sedimentation rates drastically decreased, gradients steepened, and sediments coarsened. In the final phase, basinwide sedimentation was brought to an end starting after ca. 0.16 Ma, when the Awash River incised rapidly and deeply, carving out the dramatic badlands seen today.

Adu-Asa Formation

The Adu-Asa Formation presents a sharp contrast to other periods of basin filling in that basaltic volcanism dominates over sedimentation. Accumulation rates appear to be fairly high (Fig. 12), but sedimentation occurred in small-scale rivers in narrow, probably north-south-oriented valleys. The dominantly basaltic composition of the Adu-Asa Formation (termed the Dahla Series Basalts by the volcanologic literature) is thought to mark the replacement of continental crust by incipient oceanic crust (Wolfenden et al., 2005) under the widening South Afar Rift.

The paleoenvironmental picture that emerges for the Adu-Asa Formation is one of multiple centers of eruptions, almost all basaltic but some felsic (including the Ogoti complex at Gona), covering most of the area with 3–10-m-thick flows and thin basaltic and felsic tephras (Fig. 13A). This must have been the general setting over a very large area to the south (>75 km),

since the Adu-Asa Formation is lithologically similar in the Middle Awash area (WoldeGabriel et al., 2001). The presence of paleosols between many but not all flows (Fig. 3B) shows that $>10^3$ – 10^4 yr elapsed between basaltic eruptions in many cases, if soils developed at rates similar to those on basalt flows in the southwestern United States (Laughlin et al., 1994; van der Hoven and Quade, 2002). The active volcanic areas near Nazaret in the Main Ethiopian Rift south of Gona provide clues to how such basalt-dominated landscapes may have looked. Areas on older flows with continuous soil cover are densely vegetated with C_4 grasses and to a lesser extent C_3 trees and shrubs, whereas rugged younger flows carry mainly dispersed C_3 plants.

Paleorivers threaded their way along a narrow, probably north-south depression (Fig. 13A) during much of Adu-Asa Formation deposition. The rivers clearly had extralocal sources, given the mix of felsic and basaltic clasts present in river channels, but flow directions could not be established. Small lakes developed in the older (6.2–6.4 Ma) part of the sedimentary package, laying down greenish, fissile shales and diatomites. Well-developed paleosols are unsurprisingly lacking in this environment. The floodplain was narrow and probably very active, and at times locally covered by marshes and a shallow lake. Taken together, the Adu-Asa Formation may well represent the early stages of extension, the “rift initiation stage” of Gawthorpe and Leeder (2000), in which small half-grabens were filled by sediments from small rivers and lakes, and by ongoing basaltic volcanism. However, the limits of the basin containing the Adu-Asa Formation sediments are hard to establish. The pervasive eastward dip of the Adu-Asa Formation points to rotation along a west-dipping normal fault. This fault has not been identified but would have to be located to the east, probably now buried beneath younger deposits.

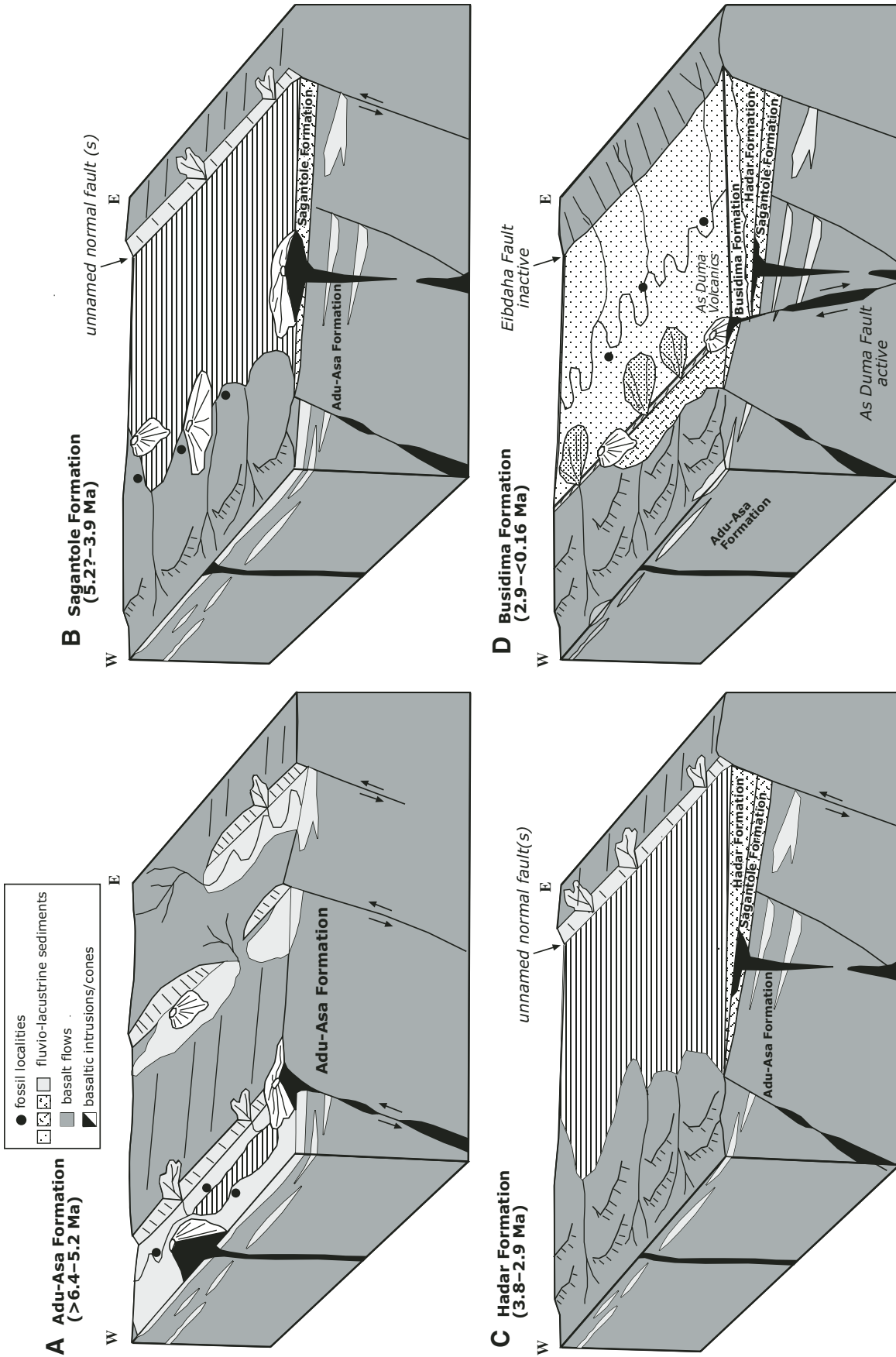


Figure 13. Tectono-stratigraphic evolution of the region for the (A) Adu-Asa, (B) Sagantole, (C) Hadar, and (D) Busidima Formations. The nature of the graben-bounding normal fault in B and C is speculative and is represented here as a single north-south-trending structure, identified as the Eibdaha fault by Dupont-Nivet et al. (this volume), or by Wynn et al. (this volume), or by Wynn et al. (this volume) as a series of unnamed normal faults. Solid dots show positions of hominid remains on paleolandscapes.

Additional key paleoenvironmental evidence for the Adu-Asa Formation comes from carbon isotopic evidence from fossil teeth (the intraflow paleosols lack soil carbonate for analysis). The carbon isotope evidence from teeth as presented in this volume (Levin et al., this volume) shows that C_4 plants (grasses) dominated the diets of most of the large herbivores (the hippopotamuses, horses, and elephants, for example), pointing to abundant grass cover somewhere in the vicinity of the water courses between basalt flows. The presence of C_3 (forest/shrubs) diet is also clearly indicated in some pigs, some bovids, and giraffes. These taxa fed in an open- rather than closed-canopy forest. Modern analogs near Nazaret would suggest that the narrow water courses were probably forested. Older basalt flows bordering the water courses were mantled by soil and covered mainly by C_4 grasses, whereas younger flows unsmoothed by pedogenesis were probably covered by very sparse C_3 trees and shrubs.

Sagantole Formation

We suggest that the Sagantole (<5.6–3.9 Ma) Formation reflects the next tectono-sedimentary stage in rifting: rapid and widespread sedimentation in a broadening and deepening of the basin. During this phase, graben-bounding faults extended and linked (Gawthorpe and Leeder, 2000), integrating the smaller Adu-Asa-age basins into a much larger one (Fig. 13B). Patterns of sedimentation and deformation give clear indications of the new basin geometry. The eastward dip of the Sagantole Formation suggests rotation along a west-dipping normal fault located somewhere east of Gona. Hence, deposition during Sagantole time was in an east-dipping half-graben. This would place Gona on the western side of the paleobasin, which is consistent with field evidence. Most of the Sagantole Formation is sedimentary at Gona, but to the north and south, these sediments interfinger with stacked basalt flows (Fig. 1). The fossil remains from the As Duma and Segala Noumou Members occur in a valley-margin setting, where lake deposits interfingered with small fluvial channels or lapped onto active basaltic cones and flows (Fig. 13B). This geometry suggests that Gona was situated at the western edge of a large lake and fluvial system in a basin that was centered to the east but is now down-faulted and buried under the Hadar Formation. Moreover, the Sagantole Formation at Gona is chopped by numerous small-scale normal faults, a distinguishing characteristic of hinge zones of half-grabens (Morley, 1995).

It is also highly likely that the lakes and rivers represented by the Sagantole Formation at Gona were linked to those farther south in the Middle Awash Project area, infilling one large “Sagantole” paleobasin or half-graben that was the immediate ancestor to the modern Awash half-graben. Sediments from the As Duma and Segala Noumou Members strongly resemble the Sagantole Formation exposed in the central complex of the Middle Awash. There, the Sagantole Formation dates between 5.6 and 3.9 Ma and is over 300 m thick (Renne et al., 1999), which is much thicker and overlaps the age of the As Duma (older than 4.6 Ma) and Segala Noumou (4.6–4.2 Ma) Members

at Gona. Large areas of the Sagantole Formation west of the Segala Noumou fault are undated and may well fill much of the time gap back to ca. 5.0 Ma. The dated Segala Noumou Member (4.6–4.2 Ma) at Gona spans the upper Haradaso (5–4.4 Ma), Aramis (4.4–4.3 Ma), and Beidareem Members (4.3–4.19 Ma) of the Sagantole Formation. All three members are lacustrine and contain an ensemble of lithologies reminiscent of those in the Segala Noumou Member (Renne et al., 1999). Our view is that this portion of the Sagantole at Gona and in the Central Complex quite possibly was deposited in a single north-south-trending “Sagantole” paleovalley (half-graben), where Gona was on the western margins of the valley bordered by basalts, and the Central Complex was closer to the paleoaxis.

Carbon isotopic evidence from carbonates in the paleosols (Levin et al., 2004; Semaw et al., 2005) and from teeth (Levin et al., this volume) points to a mix of C_3 and C_4 vegetation in the western Gona Paleoanthropological Research Project area during deposition of the Segala Noumou Member. Ten paleosol profiles and 68 samples were taken within an ~2 km radius of hominid site GWM-3 (Fig. 4). The carbon isotopic composition of soil carbonates shows that the landscape was a mixed C_3/C_4 system, but C_3 plants (trees and shrubs) dominated in the area of sampling. This, therefore, was the paleoenvironmental context in which remains of *Ardipithecus ramidus* came to be preserved.

As with the Adu-Asa Formation, carbon isotope evidence from fossil teeth of the majority of large herbivores of the Sagantole Formation shows a clear preponderance of C_4 plants (grasses) in their diet (Levin et al., this volume). This contrasts with the dominance of C_3 plants indicated by the paleosol isotopic evidence in the vicinity of the hominid sites. This suggests that the low, well-watered areas represented by much of the Sagantole Formation were dominated by C_3 plants, whereas the surrounding, slightly higher elevation areas—whether volcanic or sedimentary—were grass covered, especially where soil cover was thick. Preservation in the geologic record is always biased toward the lowest topography, a setting that would therefore be strongly represented in our paleosol record.

Hadar Formation

Depositionally, the Hadar Formation appears to represent a continuation of the fluvio-lacustrine sedimentation that started in the Sagantole Formation time, and possibly within the same half-graben (Fig. 13C). The key difference is that the extent of the paleobasin is still visible despite faulting and younger sedimentation. Combined evidence from all the project areas in the region paints a clear picture of the Hadar-age basin. Both Dupont-Nivet et al. (this volume) and Wynn et al. (this volume) report significant thickening of the Hadar Formation eastward and northward, in the direction of what we assume to be hanging-wall depocenter. The Hadar Formation also dips gently eastward, from as much as 7°E to 10°E at As Aela, 1°E at Ledi-Geraru (Dupont-Nivet et al., this volume), and up to 2°E (but with much local variation depending on fault block) at Dikika (Wynn et al., this volume).

Dupont-Nivet et al. (this volume) identify the Eibdaha fault zone on the east side of Ledi-Geraru as a possible graben-bounding fault for the Hadar basin, juxtaposing older basalts in the hanging wall against Hadar Formation in the footwall. Wynn et al. (this volume), working at Dikika, recognize the Hadar graben as bounded to the east and northeast by a series of normal faults, rather than by a single fault. The location of this graben-bounding fault is a topic for further work.

Depositional patterns are the third key line of evidence in favor of a hanging-wall depocenter on the east and northeast side of the basin, and hence a west-dipping half-graben during Hadar deposition. Through much of Hadar Formation time, the Hadar and Gona project areas lay at the southern margin of a major lake system (Tiercelin, 1986; Wynn et al., this volume) that transgressed at least three times into the Gona area. Fluvio-lacustrine and deltaic sediments dominate the Hadar Formation in both areas (Campisano and Feibel, this volume, Chapter 8). Marginal lacustrine gastropod limestone crops out as far west as As Aela. The profundal facies, and hence the deepest part of the lake, occurs well to the north and east of Gona in the Ledi-Geraru project area (DiMaggio et al., this volume; Dupont-Nivet et al., this volume). In general, sediments in the Hadar Formation are finer grained than those in the underlying Sagantole Formation and in the overlying Busidima Formation, pointing to a low-gradient, low-energy system. However, very high sedimentation rates characterize the Hadar Formation at Gona (Fig. 12; 0.25 mm/yr) and central Hadar, and rates are as much as 1 mm/yr in central Ledi-Geraru (Dupont-Nivet et al., this volume). This indicates that the valley must have been partially structurally closed at some point north of Ledi-Geraru, and that the half-graben was very actively subsiding to accommodate the influx of sediment. Closure to the north and south may have been the result of hanging-wall highs along accommodation zones (Gawthorpe and Leeder, 2000). By deposition of the BKT-2U tephra (DiMaggio et al., this volume) at 2.94 Ma, the last Hadar-age lake had regressed, probably marking the filling of the half-graben to the height of the downstream accommodation zone.

Deposition older than ca. 4 Ma was strongly influenced by basaltic volcanism, whereas the Hadar and Busidima Formations are largely sedimentary at Gona, and the tephrae are nearly all felsic, fine-grained, and probably extraregionally derived. To be sure, the As Duma fault created a conduit for the basaltic dikes, cinder cones, and flows of the As Duma volcanics, but these extrusions are very small in volume compared to the voluminous basaltic volcanism of the Sagantole and Adu-Asa Formations. Even this volcanism has slowed and apparently stopped, based on the deeply dissected nature of the cones and exhumation of the dikes. Limited basaltic volcanism also continued to the north in Hadar and Ledi-Geraru (Aronson and Taieb, 1981; Dupont-Nivet et al., this volume).

This gradual decline in volcanic activity along this sector of the southern Afar Rift is probably linked to the eastward shift and focusing of volcanism along the Wonji belt. The Wonji fault belt is a series of active volcanoes and east-stepping rift grabens

located ~100 km east of Gona (Hayward and Ebinger, 1996; Tesfaye et al., 2003). The onset of faulting along the Wonji belt is unconstrained, but the age of the oldest dated volcanic rocks is ca. 1.6 Ma (Meyer et al., 1975). This process of eastward stepping and narrowing of volcanism is part of a longer pattern extending back to the early Miocene (Wolfenden et al., 2005). The volcanic “step” out of the Gona area occurred gradually, perhaps commencing during Segala Noumou Member time (4.6–4.2 Ma), and proceeding through sometime between the end of As Duma volcanism (younger than 2.9 Ma) and beginning of Wonji Belt volcanism (younger than 1.6 Ma). Although local volcanism had ended at Gona by Hadar time, tectonism had not. The high sedimentation rates (Fig. 12; 0.25 mm/yr) displayed by the Hadar Formation are probably in part linked to active slip along the as-yet-unidentified normal fault bounding the E-NE margin of the paleobasin.

Busidima Formation

The Busidima Formation in general marks an important shift in the style of basin filling. The Busidima Formation was laid down entirely by the ancestral Awash River and its tributaries (Fig. 13D). The filling pattern was one of local downcutting by 5–15 m into older sediment, creating shallowly dissected badlands, followed by backfilling and eventual overtopping of the eroded landscape by new sediment. The backfilling was accomplished by a combination of lateral channel accretion in a meandering fluvial system, and by significant overbank flooding (Quade et al., 2004). As locally dissected areas filled with sediment, the river axis migrated laterally and paleosols developed. Average paleosol development is in general weakest in the lower Busidima Formation, where the paleo-Awash River returned every 250,000 yr, and strongest when the Awash migrated entirely out of the Gona project area toward the east. Oldowan stone tools are confined to the three oldest (2.6–1.9 Ma) channel-filling events of the paleo-Awash River, the Acheulian to at least six paleo-Awash sequences above that (1.9–1.6; and ca. 0.6 Ma), and the Late Stone Age ? (younger than 0.05 Ma) to the last filling event at the top of the section.

We agree with Wynn et al. (this volume) that major westward thickening of the Busidima Formation clearly points to deposition in a west-dipping half-graben. This is the opposite polarity of the half-graben that accommodated the Sagantole, Hadar, and probably the Adu-Asa Formations, and, as such, it represents a major new stage in the basin evolution. Such shifts in basin polarity are common in the mature stages of rift-basin evolution, whereby normal faults along previously segmented half-grabens extend and merge, leading to sedimentation over former accommodation zones (Lambiase and Bosworth, 1995).

The western boundary of the newly formed half-graben in Busidima time was the As Duma normal fault. It runs along the western half of the Gona project area, juxtaposing the Busidima Formation against the Sagantole in the south and center (Fig. 1). Northward, the As Duma fault turns NE and cuts upsection

through the Hadar Formation. This clearly shows that fault displacement commenced no earlier than 3.5 Ma, the age of the top of the As Aela section. On air photographs, the As Duma fault continues to cut upsection into the Hadar Formation. Combined with the rest of the evidence for westward thickening of the Busidima Formation (Wynn et al., this volume), the As Duma fault likely began to experience offset at some time late in Hadar Formation time. This led to the formation of the modern, west-dipping Awash graben and deposition of the Busidima Formation (Fig. 13D). Significantly, the Busidima Formation is thin to absent on the east side of Ledi-Geraru area, suggesting little or no movement along the E-NE bounding fault (the Eibdaha or other) after 2.9 Ma. We presume, therefore, that this area became the hinge zone of the Awash half-graben during Busidima time.

Other evidence strongly supports the concept of increasing interbasin linkage and sedimentary overtopping of Hadar-age accommodation zones (Gawthorpe and Leeder, 2000) in Busidima time. A fivefold decrease (0.25 versus 0.05 mm/yr) in sediment accumulation rates accompanied the conspicuous shift in depositional style from the Hadar to Busidima Formation. This indicates that much less sediment was arriving in the Awash half-graben than during Hadar time, or that more sediment was being exported from the graben than previously. In essence, the basin became a largely sediment-bypass zone, which is typical of rift basins that have overtopped accommodation zones (Lambiase, 1990). Slowing slip rates along the As Duma fault may have also contributed to lower sedimentation rates, as the most active extension shifted eastward by 1.6 Ma to the Wonji fault belt, as well as westward to the Borkena and the Dergaha-Sheket grabens. These areas today display the greatest extension rates (4.5 ± 0.1 mm/yr; Bilham et al., 1999) and seismic activity (Tesfaye et al., 2003). Having said this, a >10 m scarp marking the As Duma fault at most locations at Gona, except along active drainages, provides clear geomorphic evidence for recent movement (late Quaternary). Moreover, mid- to late Quaternary gravels resting on the As Duma volcanics are clearly offset by the As Duma fault by >4 m.

Mainly fluvial deposition, much lower sedimentation rates ($<<0.05$ mm/yr), and large-scale cutting-and-filling seem to characterize age-equivalent sediments of the Busidima Formation in other areas of the Awash basin. In the Hadar project area north of Gona, the Busidima Formation is also fluvial and only 45 m thick (Campisano et al., this volume, Chapters 6 and 8), whereas it is apparently not present at all in the middle Ledi-Geraru project area (DiMaggio et al., this volume). In the Middle Awash project area south of Gona, the Bouri Formation exposed in the Bouri Peninsula (a horst) spans about the same time period as the Busidima Formation, roughly 2.6–2.7 to 0.15 Ma (de Heinzelin et al., 1999; de Heinzelin, 2000; Clark et al., 2003). However, the total known thickness of the Bouri Formation is ~80 m, even less than the 130 m represented at Gona. Part of the reason is that up to 1.5 m.y. (2.5–1.0 Ma) of the sedimentary record appears to be missing at Bouri. The Bouri Formation is on average much finer grained than the Busidima Formation, and it is lacustrine

for short periods, pointing to local structural impoundment (an accommodation zone?) such as that which occurs today by the Bouri horst. The dominantly fluvial nature of deposition at this time is seen closer to Gona in the eastern Middle Awash area (Williams et al., 1986).

In summary, the weight of the regional evidence during Busidima deposition shows many of the key features of the “through-going fault stage” of rift basins (Lambiase, 1990; Gawthorpe and Leeder, 2000). Consistent with this phase of evolution of most rifts: (1) lacustrine sedimentation in more localized basins during Hadar time and before was replaced with major axial drainage by a through-going river in Busidima time; (2) sedimentation rates sharply decreased due to decreased extension rates, possibly combined with partial hydrographic opening of the lower reaches of the basin north of Ledi-Geraru, draining the final Hadar-age lake dated at ca. or older than 2.94 Ma. This would have permitted greater net export of sediment from the basin. (3) Exposures show near-vertical stacking of axial channel belts adjacent to footwall fans, and (4) periodic (1.0–0.5 Ma) large-fan forcing of the axial river away from the footwall. The modern analog for this mature stage in rifting is the Rio Grande River, which flows along the Rio Grande Rift in the southwestern United States (Cavazza, 1986; Lambiase and Bosworth, 1995).

A very large sample of paleosols and over 285 carbon isotope analyses (Levin et al., 2004; Quade and Levin, 2008) from the lower Busidima Formation reveal a range of abundance of C_4 plants from nearly pure forest in a few settings to open grassland in others, for an average of ~50–50 mix of C_3 and C_4 plants for this portion of the formation. Detailed sampling along single paleosols reveals a vegetation pattern very similar to that seen across the floodplain of the modern Awash River, in which gallery forest grows in a narrow band along the active Awash channel, and swards of tall edaphic grasslands grading to *Acacia*-shortgrass savanna cover alluvial fans marginal to this. Isotopic evidence for nearly pure grassland first occurs at the base of the formation in a few samples, among the earliest evidence for a savanna ecosystem in East Africa. The proportion of C_4 grasses increases slightly to 60% in the upper Busidima Formation, in both the type I and type II lithofacies, similar to the mix of plant types seen across Gona today (Quade and Levin, 2008).

Late Quaternary Incision

Carving of the badlands at Gona by deep incision of the Awash River is a young event and arguably the most significant geomorphic event in the area since the beginning (2.7 Ma) of Busidima Formation time. The minor cutting-and-filling events (≤ 35 m) of the Busidima Formation bear no comparison to the deep (>250 m) incision that produced the modern valley. When and why did this incision occur?

The beginning of incision has yet to be worked out in detail, but we estimate that it started sometime in the last 160,000 yr. The main basis for this is the presence of the Waidedo Vitric Tephra (0.16 Ma) near the top of the Busidima Formation, along

the upper Asbole. The presence of Late (?) Stone Age artifacts at YAS-1 (Fig. 10), in association with a paleo-Awash River high on the western side of the valley (Fig. 10), would suggest an even younger age (younger than 0.05 Ma) of incision, although detailed archaeological studies of the site have yet to be conducted. Another interesting clue to the downcutting history is the presence of the Butte tephra (Table 4) in inset paleochannels of the paleo-Awash River 40–75 m above the modern Awash River. Eventual dating of this tephra should fix the height of the recently incising paleo-Awash River at those times.

The causes for this unprecedented incision remain speculative. The explanation for incision that we favor is base-level drop of the Awash River in its lower reaches. Satellite photos suggest that the modern Awash River is deeply incised as far downstream as the Karrayu graben northeast of the Ledi-Geraru Project area (see Fig. 1 of volume introduction). Base-level lowering as this graben developed may be the key to the recent dramatic incision of the Awash River. The Karrayu graben is clearly an active part of the complex interaction of triple-junction tectonics, but its history is undocumented. Further downstream, the Awash River terminates in Lake Abhe, which occupies the Goba'ad graben, after passing through the Tendaho-Goba'ad discontinuity (see preface, this volume) bordering the southern side of the graben. The Goba'ad graben is a young feature dating to younger than 2.5 Ma (Gasse, 1990). Some studies (Courtillet et al., 1980; Tesfaye et al., 2003) connect the activation of Goba'ad and other east-west grabens with recent eastward propagation of the Gulf of Aden Rift into the southern Afar region. Major subsidence of these grabens sometime prior to ca. 200 ka may also have played a role in recent Awash River incision.

Tectonic versus Climatic Controls on Sedimentation

Gona provides a well-dated example of the tectono-sedimentary evolution of rifts. In accordance with models (Lambiase, 1990; Gawthorpe and Leeder, 2000) of this process, the record from Gona and surrounding areas displays a long-term coarsening-upward sequence, in which basal fluvial and minor lacustrine deposits (Adu-Asa Formation) grade upward into fine-grained lacustrine deposits (Sagantole and Hadar Formations), and into the coarse fluvial deposits of the Busidima Formation on top. Each stage in the rifting process lasted 1–3 m.y. The earliest “fault initiation” stage represented by the Adu-Asa Formation lasted a minimum of 1.2 m.y. (>6.4–5.2 Ma). The Sagantole (>4.6–3.9 Ma) and Hadar Formations (3.8–2.9), representing the “interaction and linkage stage,” lasted 1.7–2.1 m.y. The final “through-going fault stage” exemplified by the Busidima Formation lasted ~2.5 m.y. (2.7 to <0.16 Ma). Models also describe a final “fault death” stage (Gawthorpe and Leeder, 2000) in which extension ceases, but this stage does not appear to have developed yet at Gona, given the clear evidence of significant recent activity along the As Duma fault. Rather, sedimentation appears to have ceased in the basin because of propagation of the rift triple junction westward, capturing the lower Awash

and causing a base-level drop of the system that has only very recently (younger than 0.16 Ma) propagated into the Gona area.

From the foregoing, we clearly take the view that tectonics dominates over climate in determining the nature of basin deposition on long (10^6 yr) timescales. Recently, Trauth et al. (2005) suggested that East Africa experienced at least three wet phases during the last 2.7 Ma, based on the grouping of lake deposits at 2.7–2.5, 1.9–1.7, and 1.1–0.9 Ma in many sections across the region. This is the time spanned by the Busidima Formation, and, as we have pointed out, no lakes were present during this time in the northern Awash area. The reason is obvious: there must be a hydrographically closed basin to contain a lake. Development of a large, geologically conspicuous lake depends vitally on the tectonic stage of development of the basin, when extension rates are high and accommodation zones are not overtopped by sediment. The modern Awash valley is a cautionary example of the fundamental role of tectonics in lake formation. The Awash graben is terminated to the south in the Middle Awash Project area by the Bouri horst (see introduction), which represents an accommodation zone extending east from the Ayelu volcanic center. The only lake present in the valley, Yardi Lake, is dammed by uplift of the Bouri horst transverse to the main valley axis (de Heinzelin et al., 1999). It would be misplaced to use these deposits from a tectonically produced lake to deduce a wet climatic phase.

ACKNOWLEDGMENTS

The staff of the Gona Paleoanthropological Research Project would like to thank the Authority for Research and Conservation of Cultural Heritage of the Ministry of Culture and Tourism and the National Museum of Ethiopia for the research permit and general support. We appreciate K. Schick and N. Toth at the Stone Age Institute for their overall support. The L.S.B. Leakey Foundation, National Geographic Society, Wenner-Gren Foundation, and the National Science Foundation (NSF) funded this research, as did Tim White and the late Clark Howell through the Revealing Hominid Origins Initiative (RHOI-NSF) program (Division of Behavioral and Cognitive Sciences Award no. 0321893). We appreciate the hospitality of Culture and Tourism of the Afar Regional State at Semera and our Afar colleagues at Eloha. Fieldwork participants included Ali Ma'anda Datto, Ibrahim Habib (deceased), Asahamed Humet, and Yasin Ismail Mohamed. Melanie Everett, Steve Frost, Bill Hart, Lisa Peters, Mike Rogers, and Dietrich Stout are all warmly acknowledged for their help. We owe Matt Heizler a special thanks for providing so much help. We also acknowledge Berhane Asfaw, Yonas Beyene, Giday WoldeGabriel, Asahmed Humer, Alemu Admasu, and Menkir Bitew.

REFERENCES CITED

- Aronson, J.L., and Taieb, M., 1981, Geology and paleogeography of the Hadar hominid site, Ethiopia, *in* Rapp, G., and Vondra, C.F., eds., *Hominid Sites: Their Geologic Settings*: Boulder, Colorado, Westview Press, p. 165–195.

- Aronson, J.L., Schmitt, T.J., Walter, R.C., Taieb, M., Tiercelin, J.J., Johanson, D.C., Naeser, C.W., and Nairn, A.E.M., 1977, New geochronologic and paleomagnetic data for the hominid-bearing Hadar Formation of Ethiopia: *Nature*, v. 267, p. 323–327, doi: 10.1038/267323a0.
- Aronson, J.L., Vondra, C.F., Yemane, T., and Walter, R., 1996, Character of the disconformity in the upper part of the Hadar Formation: *Geological Society of America Abstracts with Programs*, v. 28, no. 6, p. 28.
- Bilham, R., Bendick, R., Larson, K., Mohr, P., Braun, J., Tesfaye, S., and Asfaw, L., 1999, Secular and tidal strain across the main Ethiopian Rift: *Geophysical Research Letters*, v. 26, no. 18, p. 2789–2792, doi: 10.1029/1998GL005315.
- Bosworth, W.P., 1985, Geometry of propagating continental rifts: *Nature*, v. 316, p. 625–627, doi: 10.1038/316625a0.
- Butler, R.F., 1992, Paleomagnetism: Magnetic domains to geologic terranes: Boston, Blackwell Scientific Publications, p. 83–104.
- Campisano, C.J., and Feibel, C.S., 2008, this volume (Chapter 6), Tephrostratigraphy of the Hadar and Busidima Formations at Hadar, Afar Depression, Ethiopia, in Quade, J., and Wynn, J.G., eds., *The Geology of Early Humans in the Horn of Africa: Geological Society of America Special Paper 446*, doi: 10.1130/2008.2446(06).
- Campisano, C.J., and Feibel, C.S., 2008, this volume (Chapter 8), Depositional environments and stratigraphic summary of the Pliocene Hadar Formation at Hadar, Afar Depression, Ethiopia, in Quade, J., and Wynn, J.G., eds., *The Geology of Early Humans in the Horn of Africa: Geological Society of America Special Paper 446*, doi: 10.1130/2008.2446(08).
- Cavazza, W., 1986, Sedimentation pattern of rift-filling unit, Tesuque Formation (Miocene), Espanola Basin, Rio Grande Rift, New Mexico: *Journal of Sedimentary Petrology*, v. 59, p. 287–296.
- Chernet, T., Hart, W.K., Aronson, J.L., and Walter, R.C., 1998, New age constraints on the timing of volcanism and tectonism in the northern Main Ethiopian Rift southern Afar transition zone (Ethiopia): *Journal of Volcanology and Geothermal Research*, v. 80, p. 267–280, doi: 10.1016/S0377-0273(97)00035-8.
- Clark, J.D., de Heinzelin, J., Schick, K.D., Hart, W.K., White, T.D., WoldeGabriel, G., Walter, R.C., Suwa, G., Asfaw, B., Vrba, E., and Haile-Selassie, Y.T.D., 1994, African *Homo erectus*: Old radiometric ages and young Oldowan assemblages in the middle Awash Valley, Ethiopia: *Science*, v. 264, p. 1907–1909.
- Clark, J.D., Beyene, Y., WoldeGabriel, G., Hart, W.K., Renne, P.R., Gilbert, H., Defleur, A., Suwa, G., Katoh, S., Ludwig, K.R., Bolserrie, J.-R., Asfaw, B., and White, T.D., 2003, African *Homo erectus*: Old radiometric ages and young Oldowan assemblages in the middle Awash Valley, Ethiopia: *Science*, v. 423, p. 747–752.
- Courtillet, V., Galdeano, A., and Le Mouel, J.L., 1980, Propagation of an accreting plate boundary: Discussion of new aeromagnetic data in the Gulf of Tadjurah and the southern Afar: *Earth and Planetary Science Letters*, v. 47, p. 144–160, doi: 10.1016/0012-821X(80)90113-2.
- de Heinzelin, J., 2000, Chapter 3: Stratigraphy, in de Heinzelin, J., Clark, J.D., Schick, K.D., and Gilbert, W.H., eds., *The Acheulian and the Plio-Pleistocene Deposits of the Middle Awash Valley, Ethiopia: Royal Museum of Central Africa (Belgium) Annales-Sciences Géologiques*, v. 104, p. 11–46.
- de Heinzelin, J., Clark, J.D., White, T., Hart, W., Renne, P., WoldeGabriel, G., Beyene, Y., and Vrba, E., 1999, Environment and behavior of 2.5-million-year-old Bouri hominids: *Science*, v. 284, p. 625–629, doi: 10.1126/science.284.5414.625.
- DiMaggio, E.N., Campisano, C.J., Arrowsmith, J.R., Reed, K.E., Swisher, C.C., III, and Lockwood, C.A., 2008, this volume, Correlation and stratigraphy of the BKT-2 Volcanic Complex in west-central Afar, Ethiopia, in Quade, J., and Wynn, J.G., eds., *The Geology of Early Humans in the Horn of Africa: Geological Society of America Special Paper 446*, doi: 10.1130/2008.2446(07).
- Dupont-Nivet, G., Sier, M., Campisano, C.J., Arrowsmith, R., DiMaggio, E., Reed, K., Lockwood, C., Franke, C., and Hüsing, S., 2008, this volume, Magnetostratigraphy of the eastern Hadar Basin (Ledi-Geraru research area, Ethiopia) and implications for hominin paleoenvironments, in Quade, J., and Wynn, J.G., eds., *The Geology of Early Humans in the Horn of Africa: Geological Society of America Special Paper 446*, doi: 10.1130/2008.2446(03).
- Fisher, R.A., 1953, Dispersion on a sphere: *Proceedings of the Royal Society of London*, ser. A, v. 217, p. 295–305, doi: 10.1098/rspa.1953.0064.
- Gasse, F., 1990, Tectonic and climatic controls on lake distribution and environments in Afar from Miocene to present, in Kaz, B., ed., *Lacustrine Exploration: Case Studies and Modern Analogues: American Association of Petroleum Geologists Memoir 50*, p. 19–41.
- Gawthorpe, R.L., and Leeder, M.R., 2000, Tectono-sedimentary evolution of active extensional basins: *Basin Research*, v. 12, p. 195–218, doi: 10.1046/j.1365-2117.2000.00121.x.
- Gentry, A.W., 1981, Notes on Bovidae (Mammalia) from the Hadar Formation and from Amado and Geraru, Ethiopia: *Kirtlandia*, v. 33, p. 1–30.
- Geraads, D., Alemseged, Z., Reed, D., Wynn, J., and Roman, D.C., 2004, The Pleistocene fauna from Asbole, lower Awash Valley, Ethiopia, and its environmental and biochronological implications: *Geobios*, v. 37, p. 697–718, doi: 10.1016/j.geobios.2003.05.011.
- Haileab, B., and Brown, F.H., 1994, Tephra correlations between the Gadeb prehistoric site and the Turkana Basin: *Journal of Human Evolution*, v. 26, p. 167–173, doi: 10.1006/jhev.1994.1009.
- Hayward, N.J., and Ebinger, C.J., 1996, Variations in the along-axis segmentation of the Afar Rift system: *Tectonics*, v. 15, no. 2, p. 244–257, doi: 10.1029/95TC02292.
- Hunt, J.B., and Hill, P.G., 1993, Tephra geochemistry: A discussion of some persistent analytical problems: *The Holocene*, v. 3, no. 3, p. 271–278, doi: 10.1177/095968369300300310.
- Johanson, D.C., and Taieb, M., 1976, Plio-Pleistocene hominid discoveries in Hadar, Ethiopia: *Nature*, v. 260, p. 293–297, doi: 10.1038/260293a0.
- Johanson, D.C., Taieb, M., and Coppens, Y., 1982, Pliocene hominids from the Hadar Formation, Ethiopia (1973–1977): Stratigraphic, chronologic, and paleoenvironmental contexts, with notes on hominid morphology and systematics: *American Journal of Physical Anthropology*, v. 57, p. 373–402, doi: 10.1002/ajpa.1330570402.
- Kalb, J.E., Oswald, E.B., Tebedge, S., Mebrate, A., Tola, E., and Peak, D., 1982, Geology and stratigraphy of Neogene deposits, middle Awash Valley, Ethiopia: *Nature*, v. 298, p. 17–25, doi: 10.1038/298017a0.
- Kimbel, W.H., Johanson, D.C., and Rak, Y., 1994, The first skull and other new discoveries of *Australopithecus afarensis*: *Nature*, v. 368, p. 449–451, doi: 10.1038/368449a0.
- Kirschvink, J.L., 1980, The least-squares line and plane and the analysis of palaeomagnetic data: *Geophysical Journal of the Royal Astronomical Society*, v. 62, p. 699–718.
- Kleinsasser, L.L., Quade, J., McIntosh, W.C., Levin, N.E., Simpson, S.W., and Semaw, S., 2008, this volume, Stratigraphy and geochronology of the late Miocene Adu-Asa Formation at Gona, Ethiopia, in Quade, J., and Wynn, J.G., eds., *The Geology of Early Humans in the Horn of Africa: Geological Society of America Special Paper 446*, doi: 10.1130/2008.2446(02).
- Lambiase, J.J., 1990, A model for tectonic control of lacustrine stratigraphic sequences in continental rift basins, in Kaz, B., ed., *Lacustrine Exploration: Case Studies and Modern Analogues: American Association of Petroleum Geologists Memoir 50*, p. 265–276.
- Lambiase, J.J., and Bosworth, W., 1995, Structural controls on sedimentation in continental rifts, in Lambiase, J.J., ed., *Hydrocarbon Habitat in Rift Basins: Geological Society of London Special Publication 80*, p. 117–144.
- Laughlin, A.W., Poths, J., Healy, H.A., Reneau, S., and WoldeGabriel, G., 1994, Dating of Quaternary basalts using cosmogenic ^3He and ^{14}C methods with implications of excess ^{40}Ar : *Geology*, v. 22, p. 135–138, doi: 10.1130/0091-7613(1994)022<0135:DOQBUT>2.3.CO;2.
- Levin, N.E., Quade, J., Simpson, S., Semaw, S., and Rogers, M., 2004, Isotopic evidence for Plio-Pleistocene environmental change at Gona, Ethiopia: *Earth and Planetary Science Letters*, v. 219, p. 93–100, doi: 10.1016/S0012-821X(03)00707-6.
- Levin, N.E., Simpson, S.W., Quade, J., Cerling, T.E., and Frost, S.R., 2008, this volume, Herbivore enamel carbon isotopic composition and the environmental context of *Ardipithecus* at Gona, Ethiopia, in Quade, J., and Wynn, J.G., eds., *The Geology of Early Humans in the Horn of Africa: Geological Society of America Special Paper 446*, doi: 10.1130/2008.2446(10).
- Lourens, L.J., Hilgen, F.J., Laskar, J., Shackleton, N.J., and Wilson, D.S., 2004, The Neogene Period, in Gradstein, F.M., Ogg, J.G., and Smith, A.G., eds., *A Geologic Timescale 2004: Cambridge, Cambridge University Press*, p. 409–440.
- Lynn, W., and Williams, D., 1992, The making of a Vertisol: *Soil Survey Horizons*, v. 33, p. 45–50.
- McDougall, I., 1985, K-Ar and $^{40}\text{Ar}/^{39}\text{Ar}$ dating of the hominid bearing Plio-Pleistocene sequence at Koobi Fora, Lake Turkana, northern Kenya:

- Geological Society of America Bulletin, v. 96, no. 2, p. 159–175, doi: 10.1130/0016-7606(1985)96<159:KAADOT>2.0.CO;2.
- McIntosh, W.C., and Chamberlin, R.M., 1994, $^{40}\text{Ar}/^{39}\text{Ar}$ geochronology of middle to late Cenozoic ignimbrites, mafic lavas, and volcanoclastic rocks in the Quemado region, New Mexico: New Mexico Geological Society Guidebook, v. 45, p. 165–185.
- Meyer, W., Pilger, A., Rosler, A., and Stets, J., 1975, Tectonic evolution of the northern part of the Main Ethiopian Rift in southern Ethiopia, *in* Pilger, A., and Rosler, A., eds., Afar Depression of Ethiopia: Stuttgart, Schweizerbart, p. 352–362.
- Miall, A.D., 1978, Lithofacies types and vertical profile models in braided river deposits: A summary, *in* Miall, A.D., ed., Fluvial Sedimentology: Canadian Society of Petroleum Geology Memoir 5, p. 597–604.
- Morley, C.K., 1995, Developments in the structural geology of rifts over the last decade and their impact on hydrocarbon exploration, *in* Lambiase, J.J., ed., Hydrocarbon Habitat in Rift Basins: Geological Society of London Special Publication 80, p. 1–32.
- Nielsen, C.H., and Sigurdsson, H., 1981, Quantitative methods for electron microprobe analysis of sodium in natural and synthetic glasses: The American Mineralogist, v. 66, p. 547–552.
- Quade, J., and Levin, N., 2008, East African hominid paleoecology: Isotopic evidence from paleosols, *in* Spohnheimer, M., Reed, K., Lee-Thorp, J., and Ungar, P., eds., Early Hominin Paleoecology: Boulder, Colorado, University Press of Colorado (in press).
- Quade, J., Levin, N., Semaw, S., Simpson, S., Rogers, M., and Stout, D., 2004, Paleoenvironments of the earliest toolmakers: Geological Society of America Bulletin, v. 116, p. 1529–1544, doi: 10.1130/B25358.1.
- Renne, P.R., Swisher, C.C., III, Deino, A.L., Karner, D.B., Owens, T., and DePaolo, D.J., 1998, Intercalibration of standards, absolute ages and uncertainties in $^{40}\text{Ar}/^{39}\text{Ar}$ dating: Chemical Geology, v. 145, no. 1–2, p. 117–152, doi: 10.1016/S0009-2541(97)00159-9.
- Renne, P.R., WoldeGabriel, G., Hart, W.K., Heiken, G., and White, T.D., 1999, Chronostratigraphy of the Mio-Pliocene Sagantole Formation, Middle Awash Valley, Afar Rift, Ethiopia: Geological Society of America Bulletin, v. 111, p. 869–885, doi: 10.1130/0016-7606(1999)111<0869:COTMPS>2.3.CO;2.
- Rogers, M.J., Feibel, C.S., and Harris, J.W.K., 1994, Changing patterns of land use by Plio-Pleistocene hominids in the Lake Turkana Basin: Journal of Human Evolution, v. 27, p. 139–158, doi: 10.1006/jhev.1994.1039.
- Roman, D.C., Campisano, C., Quade, J., DiMaggio, E., Arrowsmith, J.R., and Feibel, C., 2008, this volume, Composite tephrostratigraphy of the Dikika, Gona, Hadar, and Ledi-Geraru project areas, northern Awash, Ethiopia, *in* Quade, J., and Wynn, J.G., eds., The Geology of Early Humans in the Horn of Africa: Geological Society of America Special Paper 446, doi: 10.1130/2008.2446(05).
- Schlische, R.W., 1991, Half-graben basin filling models: New constraints on continental extensional basin development: Basin Research, v. 3, p. 123–141, doi: 10.1111/j.1365-2117.1991.tb00123.x.
- Semaw, S., Renne, P., Harris, J.W.K., Feibel, C.S., Bernor, R.L., Fessaha, N., and Mowbray, K., 1997, 2.5-million-year-old stone tools from Gona, Ethiopia: Nature, v. 385, p. 333–335, doi: 10.1038/385333a0.
- Semaw, S., Rogers, M.J., Quade, J., Renne, P., Butler, R.F., Dominguez-Rodrigero, M., Stout, D., Hart, W.S., Pickering, T., and Simpson, S.W., 2003, 2.6-million-year-old stone tools and associated bones from OGS-6 and OGS-7, Gona, Ethiopia: Journal of Human Evolution, v. 45, p. 169–177, doi: 10.1016/S0047-2484(03)00093-9.
- Semaw, S., Simpson, S.W., Quade, J., Renne, P.R., Butler, R.F., McIntosh, W.C., Levin, N., Dominguez-Rodrigo, M., and Rogers, M.J., 2005, Early Pliocene hominids from Gona, Afar, Ethiopia: Nature, v. 433, p. 301–305.
- Simpson, S.W., Quade, J., Kleinsasser, L., Levin, N., MacIntosh, W., Dunbar, N., and Semaw, S., 2007, Late Miocene hominid teeth from Gona project area, Ethiopia: Program of the Seventy-Sixth Annual Meeting of the American Association of Physical Anthropologists, v. 132, no. S44, p. 219.
- Stout, D., Quade, J., Semaw, S., Rogers, M., and Levin, N., 2005, Raw material selectivity of the earliest stone toolmakers at Gona, Afar, Ethiopia: Journal of Human Evolution, v. 48, p. 365–380, doi: 10.1016/j.jhev.2004.10.006.
- Taieb, M., Johanson, D.C., Coppens, Y., and Aronson, J.L., 1976, Geological and palaeontological background of Hadar hominid site, Afar, Ethiopia: Nature, v. 260, p. 289–293, doi: 10.1038/260289a0.
- Tesfaye, S., Harding, D.J., and Kusky, T.M., 2003, Early continental breakup boundary and migration of the Afar triple junction, Ethiopia: Geological Society of America Bulletin, v. 115, no. 9, p. 1053–1067, doi: 10.1130/B25149.1.
- Tiercelin, J.J., 1986, The Pliocene Hadar Formation, Afar Depression of Ethiopia, *in* Frostick, L.E., Renaut, R., Reid, I., and Tiercelin, J.J., eds., Sedimentation in the African Rifts: Geological Society of London Special Publication 23, p. 221–240.
- Trauth, M.H., Maslin, M.A., Deino, A., and Strecker, M., 2005, Late Cenozoic moisture history of East Africa: Science, v. 309, p. 2051–2053, doi: 10.1126/science.1112964.
- van der Hoven, S., and Quade, J., 2002, Tracing spatial and temporal variations in the sources of calcium in pedogenic carbonates in a semi-arid environment: Geoderma, v. 108, p. 259–276, doi: 10.1016/S0016-7061(02)00134-9.
- Walter, R.C., 1994, Age of Lucy and the First Family: Laser $^{40}\text{Ar}/^{39}\text{Ar}$ dating of the Denen Dora Member of the Hadar Formation: Geology, v. 22, p. 6–10, doi: 10.1130/0091-7613(1994)022<0006:AOLATF>2.3.CO;2.
- Walter, R.C., and Aronson, J.L., 1982, Revisions of K/Ar ages for the Hadar hominid site, Ethiopia: Nature, v. 296, p. 122–127, doi: 10.1038/296122a0.
- Walter, R.C., and Aronson, J.L., 1993, Age and source of the Sidi Hakoma tephra, Hadar Formation, Ethiopia: Journal of Human Evolution, v. 25, p. 229–240, doi: 10.1006/jhev.1993.1046.
- Watson, G.S., 1956, A test for randomness of directions: Monthly Notices of the Geophysical Journal of the Royal Astronomical Society, v. 7, p. 160–161.
- Williams, M.A.J., Assefa, G., and Adamson, D.A., 1986, Depositional context of Plio-Pleistocene hominid-bearing formations in the Middle Awash valley, southern Afar Rift, Ethiopia, *in* Frostick, L.E., Renaut, R., Reid, I., and Tiercelin, J.J., eds., Sedimentation in the African Rifts: Geological Society of London Special Publication 25, p. 241–251.
- WoldeGabriel, G., Aronson, J.L., and Walter, R.C., 1990, Geology, geochronology, and rift basin development in the central sector of the Main Ethiopian Rift: Geological Society of America Bulletin, v. 102, p. 439–458, doi: 10.1130/0016-7606(1990)102<0439:GGARBD>2.3.CO;2.
- WoldeGabriel, G., White, T.D., Suwa, G., Renne, P., de Heinzelin, J., Hart, W.K., and Heiken, G., 1994, Ecological and temporal context of early Pliocene hominids at Aramis, Ethiopia: Nature, v. 371, p. 330–333, doi: 10.1038/371330a0.
- WoldeGabriel, G., Haile-Selassie, Y., Renne, P.R., Hart, W.K., Ambrose, S.H., Asfaw, B., Heiken, G., and White, T., 2001, Geology and palaeontology of the late Miocene Middle Awash valley, Afar Rift, Ethiopia: Nature, v. 412, p. 175–178, doi: 10.1038/35084058.
- Wolfenden, E., Ebinger, C., Yirgu, G., Renne, P.R., and Kelley, S.P., 2005, Evolution of a volcanic rifted margin: Southern Red Sea, Ethiopia: Geological Society of America Bulletin, v. 117, no. 7/8, p. 846–864, doi: 10.1130/B25516.1.
- Wynn, J.G., Roman, D.C., Alemseged, Z., Reed, D., Geraads, D., and Munro, S., 2008, this volume, Stratigraphy, depositional environments, and basin structure of the Hadar and Busidima Formations at Dikika, Ethiopia, *in* Quade, J., and Wynn, J.G., eds., The Geology of Early Humans in the Horn of Africa: Geological Society of America Special Paper 446, doi: 10.1130/2008.2446(04).
- Yemane, T., 1997, Stratigraphy and Sedimentology of the Hadar Formation, Afar, Ethiopia [Ph.D. thesis]: Ames, Iowa State University, 182 p.

